Copyright page: This page is required for the library copy and should be inserted at the very front of your honors paper. Do not number this page. It should say:

I give permission for public access to my thesis and for copying to be done at the discretion of the archives librarian and/or the College library.

_____ _____

Signature Date

PROTEASE ACTIVITY IN LYMPHOID ORGANS OF BALB/C AND C57BL/6 MICE FOLLOWING MURINE LEUKEMIA VIRUS INFECTION

By

Tricia Lynn Nardiello

A Paper Presented to the

Faculty of Mount Holyoke College in

Partial Fulfillment of the Requirements for

The Degree of Bachelors of Arts

with Honor

Department of Biological Sciences

South Hadley, MA 01075

May 2007

This paper was prepared

under the direction of

Professor Sharon Stranford

for ten credits

For my family, thank you for your unwavering support.

My friends, who made the past four years priceless.

With love,

Tricia

ACKNOWLEDGMENTS

First of all, I would like to thank Professor Stranford for her guidance over the past four years, and her support intellectually and personally. My four years have been accentuated with priceless memories and experiences while working in your lab, thank you again. I also would like to thank Professor Bacon for her continual help with the immunofluorescence aspect of my project, your help and insight was invaluable. Professor Rachootin, you have been more than an advisor these past four years, thank you for your guidance.

I would like to extend a special thanks to my lab partner of four years, Josephine Giles, with out you during those long hours in the lab this would not have been possible. I would also like to thank all my friends that have supported me during these four years, especially Lesley Welsh and Dery Miller, your support and understanding kept me grounded.

Most of all I want to thank my family. Mom and Dad, you two have given me opportunities that you never had and I can not thank you enough. Your guidance, support, and love has helped me through these past four years and beyond. Melissa and Steven, you two are undeniably my favorites. You guys have helped me in so many ways, thank you. Thank you to my entire family for their support and confidence.

TABLE OF CONTENTS

LIST OF FIGURES

LIST OF TABLES

ABSTRACT

Current HIV research uses murine leukemia virus (MuLV) as a mouse model. There are two strains of mice that are used for this study, BALB/c and C57 BL/6. Both strains of mice will be infected with the virus, but the BALB/c mice recover while the BL/6 mice become immunocompromised (MAIDS). Previous DNA microarray work comparing the two strains has shown that certain proteases are up regulated in the BALB/c mice, in the lymph nodes and spleen. Lymphatic remolding and cell activation are possible consequences of protease activity, and it is believe that the up regulation of these proteases in the BALB/c strain may be important for recovery.

Using immunofluorescence and *in situ* zymography, visualization and quantification of protease activity in the lymph node of each strain was studied. This allowed for the fluorescent visualization of proteases within serial sections of the organ. Serial sections were stained for lymphatic (LYVE-1) and vascular (CD31) structures using primary and fluorescent secondary antibodies. This assisted in locating the proteases and revealing overall lymphatic morphology in conjunction with the protease location.

Results suggest that there is an increase in protease activity in C57BL/6 mouse strain when compared to BALB/c mouse strain in the lymph nodes. Furthermore, immunofluorescent data shows an increase in the vascular and lymphatic branching within the C57BL/6 lymph nodes.

INTRODUCTION

It is estimated by UNAIDS/WHO 2006 AIDS Epidemic Update, that 39.5 million people are living with HIV (Topor et al, 2006). There were 4.3 million new infections in 2006 with 2.8 million (65%) of these occurring in sub-Saharan Africa. Also, there have been substantial increases in Eastern Europe and Central Asia where there are some indications that infection rates have increased by more than 50% since 2004 (Topor et al, 2006). In 2006, 2.9 million people died of AIDS-related illnesses (Topor et al, 2006). This disease occurs predominately in young adults, causing large holes in the economic and social structure of many communities, especially those in Sub-Saharan Africa. The world's need for an effective treatment to this disease is becoming more critical by the day.

As of today there is still not a cure or a vaccine for HIV infections. The human immune system responds uniquely to each strain of HIV, and there is a push towards trying to differentiate between individual responses and overall trends. The way an individual's immune system reacts to HIV can determine whether they will become a long-term non progresser, who may live a healthy life with the virus for over 20 years, or a short-term progresser, who may develop AIDS within months of contracting the virus (Toper et al, 2006). This disparity in the human immune response is why it is so important to better understand the anti-

HIV immune response, to one day compensate for what the human immune system cannot do on its own.

Due to the dangers of working with HIV directly, many researchers use a mouse model to relate to the human immune system. The mouse AIDS model (MAIDS) utilizes the murine leukemia virus (MuLV). The system is unique due to the two mouse strains within the model that differ in susceptibility. C57BL/6 (BL/6) mice are similar to the short-term progressors who develop AIDS soon after contracting the virus. This mouse strain will become infected with the virus but will not be able to effectively clear it from their system. After several weeks they will become immune compromised and succumb to opportunistic infections. BALB/c mice, on the other hand, are similar to the long-term non-progressors, except they go a step further and eradicate the virus from their system completely (Liang et al, 1996).

Previous work done by S. Tepsuporn in the Stranford laboratory at Mount Holyoke College used a microarray to compare the actively transcribed genes in the lymph nodes of each mouse strain 3 days post-infection (Tepsuporn, 2005). She identified several different protease genes as upregulated in the lymph node and spleen of the BALB/c mouse strain 3 days post infection. This research follows up on her work and specifically compares protease activity at the protein level in the lymph nodes of each mouse strain at that time point. Lymphatic remolding and cell activation are consequences of protease activity (Sun and Zhang,

2006), and an increase in lymphatic vessels would allow for an increase in immune cell circulation, activation, and control of an infection. I propose that the upregulation of these proteases may cause lymphatic remolding, contributing to the recovery of the BALB/c mouse strain after MuLV infection.

I. Murine AIDS *versus* human AIDS

One way the scientific community attacks human diseases is by first studying them in animals. This allows scientists to observe the model immune system's ability to either contain the infection or its mistakes that lead to the spread of the infection. From these observations and carefully designed experiments we can correlate the human immune system with the model's and begin to fix our shortcomings. Use of the murine AIDS model system induced by the Murine Leukemia Virus (MuLV), allows for this comparison of humans and mice in an HIV animal model system (Liang et al, 1996).

Similar to HIV induced AIDS, MuLV is a retrovirus that induces massive lymphoproliferation, decreased T and B cell responses, and B cell lymphomas in some mouse strains (Kim et al, 1994). In our lab, we study two strains of mice in this model system, BALB/c and C57BL/6. Both strains become infected with the virus, however, after two weeks only the

BALB/c mice recover. The BL/6 animals experience disease progression and after 12 weeks develop an immune deficiency disorder (Hartley et al, 1989). As a result of lacking completely functional immune systems, these animals are susceptible to opportunistic infections that they would normally be able to overcome, therefore making the infections life threatening.

There are some differences between the two immune deficiency causing viruses, aside from the hosts. Although both viruses are retroviruses, MuLV is a C-type retrovirus in the oncornavirus family, while HIV is a lentivirus (Liang et al, 1996). Furthermore, HIV initially targets CD4+ T-cells and macrophages, whereas MuLV targets B-cells and macrophages (Kim et al, 1994). Even after taking all these differences into account, the MAIDS model is still considered a good model for HIV research. MuLV is safe and easy to work with for undergraduates because it is not transmittable to humans nor is it easily transmittable between mice. MuLV causes disease quickly with very consistent and dependable immunological symptoms (Liang et al, 1996). Additionally, the fact that the mouse is a well known and studied research animal with its entire genome sequenced is very helpful when looking at immunologic differences.

II. Retrovirus life cycle

Viruses are obligate intracellular pathogens, which mean that they need host cells to live. The retrovirus life cycle is very similar to most viral life cycles and it occurs completely within the host's cell. Below is a brief summary of a retroviral life cycle as described by Coffin et al. (1979). A retrovirus' nucleic acid genome is enclosed in two layers of protein, an outer capsid and an inner protein core. A retrovirus is classified by its RNA genome, which is why retroviruses also contain reverse transcriptase enzymes. These enzymes are needed to convert their RNA genome into DNA that can be compatible with the host's genome, allowing insertion to be performed.

A virus must first locate its target cell for replication. The virus binds to the plasma membrane of the host cell using viral and host cell receptors. To gain entry into the cell, the viral envelope will fuse with the plasma membrane or be endocytosed by the cell. Once inside, the viral genome will be ejected into the cytoplasm and undergo reverse transcription by the viral RNA-dependent DNA polymerase. This will convert the viral RNA into double stranded DNA that can be transported to the nucleus and integrated into the host's DNA. Once inserted into the genome, viral RNA and protein will be synthesized and sent into the cytoplasm; once enough of the proteins have been produced new virions will bud off using part of the host cell's plasma membrane. An excessive

amount of viral replication and budding off can cause a cell to lyse. Figure 1 is an illustration of a typical retroviral life cycle.

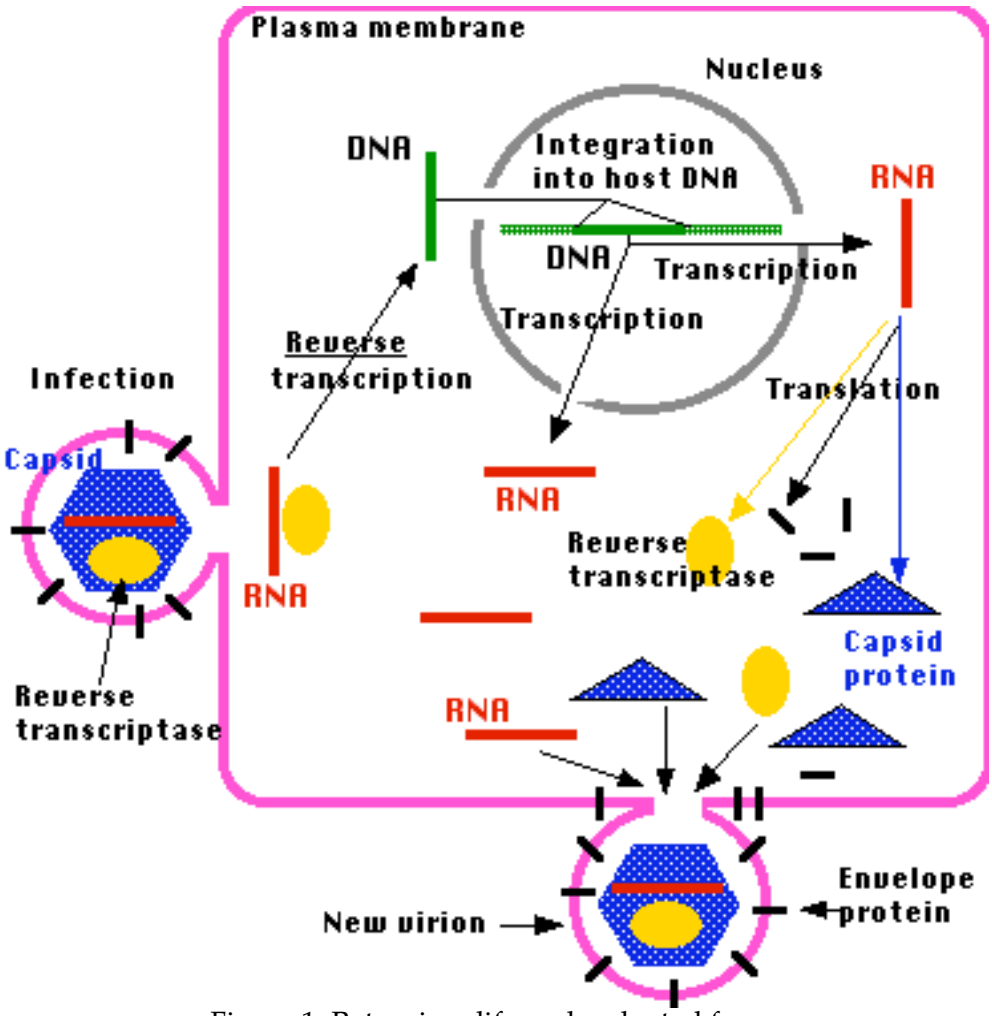

Figure 1. Retrovirus life cycle adapted from:
http://users.rcn.com/jkimball.ma.ultranet/BiologyPages/R/Retroviruses.html

III. Host Antiviral Immune Response

The host immune system can be divided into two main parts, innate and adaptive. The innate immune system includes all of the host's primary, non-specific defenses against any foreign pathogen (Janeway, 2006). This system includes barrier defenses such as skin, mucus membranes, and hair. Also, it includes innate immune cells such has macrophages, natural killer cells (NK), dendritic cells, complement, and mast cells (Janeway, 2006). These immune cells mainly utilize toll-like receptors (TLR) to detect broad characteristics about the pathogen, such as bacteria *versus* virus, and respond accordingly. The innate system also uses a combination of key cytokines and type I interferons (IFN-α,β) during infection. Interferons are produced by virally infected cells, while certain inflammatory and immune regulatory cytokines are up-regulated by leukocytes such as macrophages, NK cells, and dendritic cells (Janeway, 2006). These cytokines are only expressed by leukocytes and are called interleukins (IL). Examples of these include IL-1, IL-12, etc. This response to viral infection is continuous and unchanging. Every time these cells interact with a virus they have the same antiviral response that will continue until the adaptive immune response is activated and the infection is cleared.

Within the innate immune system, there are specific cells called antigen presenting cells (APCs). These cells will recognize a pathogen,

engulf it, and digest it into pieces. These pieces of the pathogen are molecules that will elicit an immune response and are called antigens (Janeway, 2006). APCs are critical in the immune response and act as the bridge between innate and adaptive systems. APCs present the antigens of a pathogen that the adaptive immune system will need to recognize.

The adaptive immune response takes about 7 days to become fully activated (Janeway, 2006). The main immune cells that are part of the adaptive immune response are T-cells and B-cells. For complete viral eradication, both humoral (B-cells) and cell-mediated (T-cells) responses are needed. B-cells will create neutralizing antibodies specific for the outer part of the virus, usually the envelope protein, which will bind to and inhibit host cell entry (Janeway, 2006). Antibodies can also induce complement, which are small molecules that can create pores in infected cell membranes causing apoptosis or signaling leukocytes to the area. Lastly, antibodies can bind to the virus and act as a beacon for phagocytic cells, alerting them to engulf and destroy the viron, a process known as opsoninzation (Janeway, 2006).

The B-cell antibody response will effectively clear extra-cellular viral infections, but the cell-mediated T-cell response is needed to clear intra-cellular viral infections. There are two main types of T-cells, CD8+ cytotoxic T-lymphocytes (CTL) and CD4+ helper T-cells (T_H). CTLs are able to eliminate virally infected host cells once their receptors recognize viral proteins on the host cell's surface (Janeway, 2006). T_H-cells, on the

other hand, will secrete specific cytokines once they are activated by an APC that will assist other cell types in the immune system. Some examples of the cytokines secreted are IL-2, interferon-gamma (IFN-γ), and tumor necrosis factor-beta (TNF-β). IL-2 induces proliferation and growth of T_H-cells and CTLs. IFN-γ inhibits viral replication in infected cells, limits viral entry into uninfected cells, and enhances the phagocytic activity of macrophages (Janeway, 2006). Lastly, TNF-β works with IFN-γ to help identify and kill infected cells (Janeway, 2006).

The combination of all these immune cells working together creates an effective immune response that will eradicate the virus from the host, and the trafficking of these cells will change the effectiveness of this response (Janeway, 2005). This is why the amount and size of lymphatic and blood vessels are important for an effective immune response. The larger the vessels and the higher their prevalence allows for an increase in the circulation of these immune cells, facilitating a quicker immune response. Proteases are involved in the growth of these vessels and can be important participants in the immune system (Frederiks and Mook, 2004).

IV. Proteases

Proteases are enzymes that cleave proteins and other enzymes. They are located throughout the body and perform many different

functions. Proteases are divided into two main classes, endopeptidases and exopeptidases (Frederiks and Mook, 2004). Endopeptidases cleave internal peptide bonds in proteins while exopeptidases cleave external peptide bonds. Exopeptidases are further divided into aminopeptidases and carboxypeptidases depending on which amino acid end is cleaved off the protein (Frederiks and Mook, 2004). All proteases are classified by the amino acid they recognize at the cleavage site, whether it is internal or external. There are 5 main groups of proteases: aspartic, cysteine, metalloproteases, serine, and threonine (Table 1).

Table 1. Examples of different types of proteases.

Classification of Protease	**Examples**
Aspartic	Cathepsins D, E, pepsin, rennin
Cysteine	Cathepsins B, L, S, K, Q, calpains, caspases
Metalloprotease	Gelatinases A, B
Serine	Plasminogen activators, plasmin, and chymase
Threonine	Proteasome hydrolases

Regulation of proteases is often done at the post-translational level, and it is the activity of this processed protein that mediates the function of the enzyme (Morse III et al, 1992). Many proteases are present in cells and tissue compartments in an inactive form. This can be a result of being synthesized as precursors that have little if any catalytic activity and need post-translational activation, or being bound to endogenous inhibitors (Boonacker et al, 2001). *In vivo* regulation of enzyme activity can be accomplished by altering the rate of their synthesis and degradation,

activation of proforms, and binding with endogenous inhibitors. This can be mediated through cell-cell interactions, environmental stimuli, and internal stimuli. Protease activation, on the other hand, can take place through proteolytic processing by specific proteases, autocatalysis, binding of cofactors, or removal of these inhibitors (Boonacker et al, 2001). The dysregulation of proteases have a variety of deleterious effects and has been linked to a number of pathological conditions including: cardiovascular and neurodegenerative diseases, arthritic diseases, infection, and cancer (Saban et al, 2007). This makes proteases very attractive therapeutic targets.

V. Proteases and the Immune System

Proteases are involved in many aspects of the immune system, especially in the early inflammatory response. Proteases can be anchored to the plasma membrane or can be soluble in the extracellular fluid (Saban et al, 2007). They can initiate or terminate signal transduction through cleaving receptors and ligands at the cellular surface. Protease-activated receptors (PARs) are a unique class of G protein-coupled receptors that carry their own ligands, which remain cryptic until unmasked by proteolytic cleavage (Saban et al, 2007). Therefore, cell- surface proteases can release or generate active ligands. Four PARs have been identified

with a wide range of proteases that can cleave and activate them, including proteases that arise from or originate in the coagulation cascade, inflammatory cells, and the digestive tract (Ossovskaya and Bunnett, 2004). PAR activation can initiate an array of signaling events in many different cell types with diverse consequences, ranging from hemostasis to pain transmission.

The inflammatory reaction is characterized by edema and granulocyte infiltration (Janeway, 2006). Serine proteases such as thrombin and trypsin are produced during tissue damage and make important contributions to tissue responses to injury, repair, cell survival, inflammation, and pain (Sun and Zhang, 2006). PAR expression is altered in response to inflammation. The standard signal transduction pathway downstream of PAR activation and coupling with various G proteins leads to the rapid transcription of genes involved in inflammation (Saban et al, 2007). The effect of PAR activation on the downstream transcriptome is still unknown, but it is known that proteases can interact with NK cells and promote inflammatory responses (Saban et al, 2007).

VI. Vascular and Lymphatic Remodeling

Angiogenesis and lymphangiogenesis are the processes of creating new blood vessels or lymphatic vessels, respectively. The growth of these

vessels is important for the immune response because they facilitate the movement of leukocytes to and from the infected area (Lieken et al, 2001). When there are increased numbers of vessels, the immune system can respond faster. The construction of a vascular network requires several steps including the release of proteases from "activated" endothelial cells. This is followed by the degradation of the basement membrane surrounding the existing vessel, migration of endothelial cells into the interstitial space, endothelial cell proliferation, and differentiation into mature blood vessels (Lieken et al, 2001). These processes are mediated by a wide range of angiogenic inducers, including growth factors, chemokines, angiogenic enzymes, endothelial specific receptors, and adhesion molecules (Lieken et al, 2001).

To initiate the formation of new capillaries, endothelial cells of existing blood vessels must degrade the underlying basement membrane and invade into the stroma of the neighboring tissue (Lieken et al, 2001). These processes of endothelial cell invasion and migration require the cooperative activity of the plasminogen activator (PA) system and matrix metalloproteinases (MMPs). There are two types of PAs, uPA and tPAs, both are serine proteases that convert plasminogen into plasmin. uPA is secreted as an inactive form that is cleaved by Factor Xlla or cathepsin B to become activated (Lieken et al, 2001). The activated form then interacts with its receptor at 'focal attachment sites' on the cell surface that stimulates signal transduction. This signal cascade leads to the induction

of cell migration and invasion. This migration is the beginning of capillary formation and will soon lead to new blood and lymphatic vessels.

Both physiological and pathological stimuli can induce leukocytes, macrophages, mast cells and platelets to secrete vascular endothelial growth factors (VEGF) and other growth-related factors (Sun and Zhang, 2006). These factors are then directly or indirectly involved in angiogenesis and lymphangiogenesis, causing endothelial cells of nearby blood and lymphatic vessels to divide, migrate, and form new vessels (Lieken et al, 2001). Among these factors, the VEGF family is the best characterized.

Table 2. VEGF Ligands and Receptors. The table below shows vascular endothelial growth factor receptors and their affiliated ligands. Also, the tissue expression and effects are shown below.

Tissue Expression	**Receptor**	**Ligand**	**Effect**
Vascular Endothelium	VEGFR-1	VEGF-A VEGF-B	Organizes blood vessels
Vascular and Lymphatic	VEGFR-2	VEGF-A VEGF-C VEGF-D VEGF-E	Activates vessel proliferation
Mostly Lymphatic	VEGFR-3	VEGF-C VEGF-D	Critical to the growth, migration, and survival of lymphatic endothelial cells and causes lymphangiogenesis

The ligands of the VEGF family include VEGF-A, VEGF-B, VEGF-C, VEGF-D and VEGF-E. All five ligands have different roles in the

process of angiogenesis and lymphangiogenesis (Sun and Zhang, 2006). Each of the VEGF-family ligands binds to one or more of three known VEGF receptors (VEGFR): VEGFR-1, VEGFR-2, and VEGFR-3. VEGFR-1 can be expressed on vascular endothelial cells and organizes blood vessels, and has a high affinity for VEGF-A and VEGF-B (Sun and Zhang, 2006). VEGFR-2 can be expressed on lymphatic and vascular endothelium. It activates blood vessel proliferation by binding to VEGF-A, VEGF-C, VEGF-D, and VEGF-E. VEGFR-3 is expressed on the vascular endothelium, but is mainly restricted to the lymphatic endothelium. VEGFR-3 binds to VEGF-C and VEGF-D, and is critical to the growth migration and survival of lymphatic endothelial cells, resulting in lymphangiogenesis (Sun and Zhang, 2006).

VII. Previous Microarray Studies

Past work done by Suprawee Tepsuporn quantified strain specific differential gene expression in mouse lymphoid organs after MuLV infection. The experiment was performed with a DNA microarray chip by adding cDNA synthesized from RNA originating from the spleen and lymph nodes of 3 day and 7 day infected mice of both strains (Tepsuporn, 2005). Her data showed that the genes: Ctrb1 (Casein kinase II, alpha 2 polypeptide), Ela2a (Elastase 2A), Prss2 (Protease, serine 2) and Prtn3

(Proteinase 3) were up-regulated 3 days after infection in the lymph node of the BALB/c mouse strain. The genes: Ela3b (Elastase 3B), Cttrb1, Cpb1, Pnlip, and Prss2 were all upregulated in the spleen 3 days post infection. These enzymes are part of the protease gene family. The goal of this research is to show this differential expression at the protein level and attempt to localize the response within the lymph node. Lymphatic remolding and cell activation are possible consequences of protease activity, and the upregulation of these proteases in the BALB/c strain may important for these immune activities, leading to the eradication of the virus and recovery from infection.

Microarray data reflects the cell's state of gene activation. Unfortunately, transcriptional activity does not necessarily reflect translational activity, meaning that although the gene may be transcribed the mRNA may not be translated into protein. Also, there is not a one to one relationship present, even if a small amount of mRNA is being translated it can encode for a large amount of protein and vice versa. This is especially a problem with proteases because in many cases they are stored in cells and tissues as a protein but in an inactive form. To differentiate between the presence of mRNA for an enzyme and activity, I used a new method called *In situ* zymography.

VIII. *In situ* Zymography

To properly quantify the activity of proteases, relying on transcriptome or mRNA data is not sufficient. Proteases, like many enzymes, often require post-translational modifications to be activated. They can lay dormant in large quantities in the presence of inhibitors or in the absence of activators. It is essential to localize and quantify actual protease activity *in situ* to determine whether the enzyme is functional. A newly designed method to detect enzymatic activity within tissue sections is '*In situ* Zymography' (Frederiks and Mook, 2004).

In situ zymography is a relatively new procedure utilizing a fluorescently quenched substrate that fluoresces once cleaved by an active protease (Frederiks and Mook, 2004). This allows for visualization of enzyme activity within frozen sections of a desired organ *versus* enzyme presence. This research utilizes a specially designed protease kit containing a casein derivative as a substrate. The substrate is heavily labeled with pH-insensitive green-fluorescent BODIPY FL, and will only fluoresce once cleaved by protease catalyzed hydrolysis (Frederiks and Mook, 2004).

It is also important to be able to identify the location of proteases in relation to structures within the tissue. To identify lymphatic and vascular structures within lymphoid organs, fluorescently conjugated

anti-Lyve-1 and anti-CD 31 antibodies, respectively, will be used on serial sections using immunofluorescence.

IX. Research Objective

Understanding the function and regulation of the immune system and its components is important for all medically applicable research. Utilizing the MAIDS model and the previous DNA microarray data, this thesis focuses on understanding the protease activity in connection with lymphangiogenesis and angiogenesis in response to a murine leukemia virus infection. As previously stated, protease activity is important in facilitating lymphangiogenesis, angiogenesis, and certain cell surface receptors during an immune response. This research tests the hypothesis that the upregulation reported in the microarray results allows for the BALB/c mouse strain to increase their lymphatic and vascular vessel systems, thereby allowing for an increase in immune efficacy. Support for this hypothesis and relating these discoveries to humans with current HIV infections can open a new pathway for antiviral therapeutics.

MATERIALS AND METHODS

I. Virus Stock Preparation

In these experiments, the murine leukemia virus mixture used was harvested from SC-1 cells (fetal mouse embryonic line) infected with the MuLV LP-BM5 virus. The SC-1 cells were obtained, uninfected, from the American Type Culture Collection. SC-1/MuLV LP-BM5 infected cells were obtained from NIH AIDS Research & Reference Reagent Program. SC-1/MuLV LP-BM5 culture procedures were adapted from NIH AIDS Research & Reference Reagent Program guidelines.

II. Animals and Injections

The experiments performed in this study used two strains of mice, BALB/c (disease-resistant) and C57BL/6 (disease-susceptible). These mice were males five to eight weeks old from Taconic, NY. The mice were cared for in the Mount Holyoke College Animal Facility according to the National Institutes of Health Guidelines for the Care and Use of Laboratory Animals. The mice were kept naïve and in individual cages until challenged with mock or MuLV infection. They were injected in the intraperitoneal cavity with 1mL of MuLV (approx. 1.3-3.44 x 10^6 plaque

forming units (pfu) of virus according to Suprawee Tepsuporn's thesis) or mock supernatant. The 'mock infection' consists of an injection containing only the sterile supernatant of the virus. This will show any immunological reactions that are due to the injection or supernatant, but not the virus itself. All the mice were sacrificed on the third day post-infection using carbon dioxide inhalation. There were two biological replicates per strain and infectivity, and four experimental replications per strain and infectivity. All protocols in this study received Institutional Animal Care and Use Committee approval and adhered to the guidelines of the National Institutes of Medicine animal care and use guidelines.

III. Lymph node Extraction and Freezing

Mice were dissected using sterile surgical tools and sterile technique. Whole lymph nodes were carefully extracted to minimize tissue damage using standard dissection methods. Mesenteric[1], inguinal[2], axillary[3], and brachial[4] lymph nodes were extracted from the mice and immediately embedded into OCT embedding medium located inside an aluminum boat. The organ was oriented properly in the aluminum boat using a dissecting pin, and then placed into a small bowl filled with

[1] Found in the mesentery of the pancreas and small intestines
[2] In the subcutaneous tissue of the groin
[3] Found at the armpit
[4] Located under the pectorals near the tricep muscle

methyl butane floating in a container of liquid nitrogen. Once the OCT turned white, the sample was completely frozen. It was then placed at 80°C until sectioning.

IV. Tissue Sectioning

The lymph nodes were left at -20°C for two hours to acclimate to the sectioning temperature. The lymph nodes were cut into 8um thin sections on a cryostat at -18°C in the Bacon laboratory at Mount Holyoke College. The sections were placed onto Superfrost charged microscope slides and allowed to air dry for 1hr at room temperature. The sections were labeled then fixed in acetone by immersion for 5 mins, dried for 3 mins at room temperature, and placed at -20°C until staining.

V. Hematoxylin and Eosin staining (H&E)

H&E staining was performed on the representative sections of lymph nodes on microscope slides. First, the sections were put in a humidity chamber for 20 minutes to acclimate to room temperature. Afterwards, the sections were placed in the following solutions: xylene for 5 mins, 100% alcohol for 3 mins, 95% alcohol for 3 min, 80% alcohol for

3 min, 70% alcohol for 3 min, water for 3 min, hematoxylin for 2 min, water to rinse, acid alcohol for 2 min, alkaline alcohol for 1 min, 70% alcohol for 3 min, eosin for 30 seconds, 95% alcohol for 1 min, 100% alcohol for 3 min, and finally xylene for 10 min. Balsam, an embedding medium, was laid on top of the section, a coverslip applied, and viewed under a light microscope.

VI. Immunofluorescent Staining

In this protocol rat anti-CD31 and rabbit anti-Lyve-1 antibodies were used as the primary antibodies. These were followed by fluorescently conjugated secondary antibodies, TRITC conjugated goat anti-rat IgG (red) and FITC conjugated goat anti-rabbit IgG (green).

The slides were brought to room temperature in a humidity chamber for 20 mins to acclimate to room temperature in preparation for the staining. Once the slides reached the desired temperature, the tissue sections were circled with clear Revlon nail polish to create a barrier. Next, the slides were blocked with blocking serum, a mixture of goat serum and 1x Tris-buffered saline (TBS), and incubated for 30 minutes at room temperature in the humidity chamber. The solution was then drained from the slides and 25 uL of primary antibody (rabbit anti-lyve-1 or rat anti-CD31) was placed on top of each section and allowed to incubate in the humidity chamber at room temperature for 1 hour. The

excess solution was poured off and the slides were washed 3 times with 1x TBS and allowed to sit for 5 mins after each wash.

Upon completion of the last wash cycle, 25 uL of fluorescently conjugated secondary antibody (either goat anti-rabbit IgG or goat anti-rat IgG) was applied to each tissue section and allowed to incubate in the humidity chamber at room temperature for another hour. From this point on the procedure was conducted in the dark and the slides were continually covered with aluminum foil. After the incubation, the excess solution was drained from the slides and subjected to another round of 3, 1x TBS wash cycles. After the excess TBS was drained off, melted glycerol gel was placed on each section and a coverslip layed on top. The slides were given 5-10 minutes to set before viewing under the inverted fluorescent microscope.

Two negative controls were used for each slide. One had only the blocking solution applied; the other only had the secondary antibody applied. This allowed us to check for tissue auto-fluorescence and nonspecific secondary antibody binding.

VII. *In situ* Zymography

This *In situ* Zymography protocol was adapted from the Frederiks laboratory (Frederiks, 2004) using the EnzChek Protease assay kit

purchased from Invitrogen. Below is a table listing the protease families recognized by the assay.

Table 3. Detection of EnzChek Protease Assay Kit from Invitrogen.

Enzyme Examples	**Protease Family**
Elastase, Type IV (porcine pancreas)	Serine Protease
Chymotrypsin, Type II (bovine pancreas)	Serine Protease
Thermolysin (B. proteolyticus rokko)	Acid Protease
Trypsin, Type IX (porcine pancreas)	Serine Protease
Papain (papaya latex)	Sulfhydryl Protease
Pepsin (porcine stomach mucosa)	Acid Protease
Elastase (Pseudomonas aeruginosa)	Metallo-protease
Cathepsin D	Acid Protease
Elastase (human leukocyte)	Serine Protease

Prior to staining, low melting temperature agarose was prepared by dissolving 1g of low melting temperature agarose in 100mL of PBS at pH 7.45 under continuous stirring and heating in a water bath (80°C). Once the solution was clear, the agarose was cooled to 60°C before used. After the agarose cooled, the casein solution (contained in the protease invitrogen kit) was reconstituted in deionized water and diluted 1:10 in the agarose solution. The negative control sample received only the agarose solution placed on top of the section, independent of the casein substrate.

Once the preparatory solutions were made, desired slides were placed into the humidity chamber for 20 mins to reach room temperature. Due to the agarose's tendency to congeal at room temperature, the rest of this protocol was conducted in the 37°C room. After incubation in the humidity chamber, 25 uL of the agarose solution was placed on each section and a coverslip (24x40mm) was applied. These sections will sat in the dark for 3 hours before pictures were taken. Since this is a continuous reaction that can not be stopped, it was beneficial to stagger starting times to account for the time required to visualize and photograph each slide.

VIII. Control Inhibitors

CALBIOCHEM protease inhibitor cocktail set I and CALBIOCHEM serine protease inhibitor cocktail set I were used for negative controls. The inhibitors were reconstituted in distilled water at 100x concentration and diluted to 1x prior to use. The slides were placed in the humidity chamber for 20 minutes to reach room temperature. Next, the slides were removed and 25 uL of the inhibitors were applied to the sections on the slide that were to serve as negative controls. All other sections received 25 uL of distilled water. Slides were incubated in the humidity chamber for 30 minutes and the excess liquid was drained off. The *In situ* zymography

procedure was continued as stated above, beginning with the application of the agar.

IX. Analysis

All microscopy was performed using the Nikon Eclipse TE2000-U inverted fluorescent microscope located in the room 9a Clapp with the Metavue data analysis program. Photographs of Lyve-1 staining were taken at an exposure time of 5000 milliseconds (ms), CD31 at 5000 ms, and Protease at 1000 ms. Pictures were taken using 4x, 6x, and 10x objectives and were also analyzed using the Metavue program. To analyze the data from an entire lymph node section, regions were hand drawn around the periphery of each field of view, and the area of multiple shots were added together during the data analysis to create a composite lymph node section.

Using these regions, thresholds were set with upper and lower limits on the counted fluorescence values. This was performed to eliminate background fluorescence and non-specific particulate fluorescence interference. Using the program, the regioned area, total fluorescence, and fluorescence intensity was recorded. For the protease assay, the fluorescence per square micrometer was calculated. For the

Lyve-1 and CD31 staining, the percent of the lymph node area covered in fluorescence was calculated.

RESULTS

The experiments performed used the two mouse strains, BALB/c and C57BL/6 testing mesenteric, inguinal, and axillary/brachial lymph nodes. The stains used were Lyve-1 (green), CD31 (red), and the protease assay (green). Table 4 below shows the combination of lymph node types, stains, mouse strains, and infectivity.

Table 4. Experimental Parameters. Below shows the strains of mice used along with the different stains and the lymph nodes tested. Lyve-1 staining shows lymphatic vessels in green, CD31 staining shows blood vessel in red, and the protease staining visualizes active proteases in green.

Strain	**Stains**	**Lymph node Types**
BALB/c MuLV & Mock infected	Lyve-1 CD31 Protease	Mesenteric Inguinal Axillary/Brachial
C57BL/6 MuLV & Mock infected	Lyve-1 CD31 Protease	Mesenteric Inguinal Axillary/Brachial

I. H&E Staining

The H&E staining was performed in order to show the tissue section morphology and integrity. Unfortunately, the procedure did not stain the sections as evenly as desired, nor did it highlight the proper morphology of the sections. Furthermore, there was a large amount of tissue tearing and overall degeneration post staining (Figure 2). The

staining procedure was attempted three times with limited success each time. Further attempts at H&E staining were abandoned.

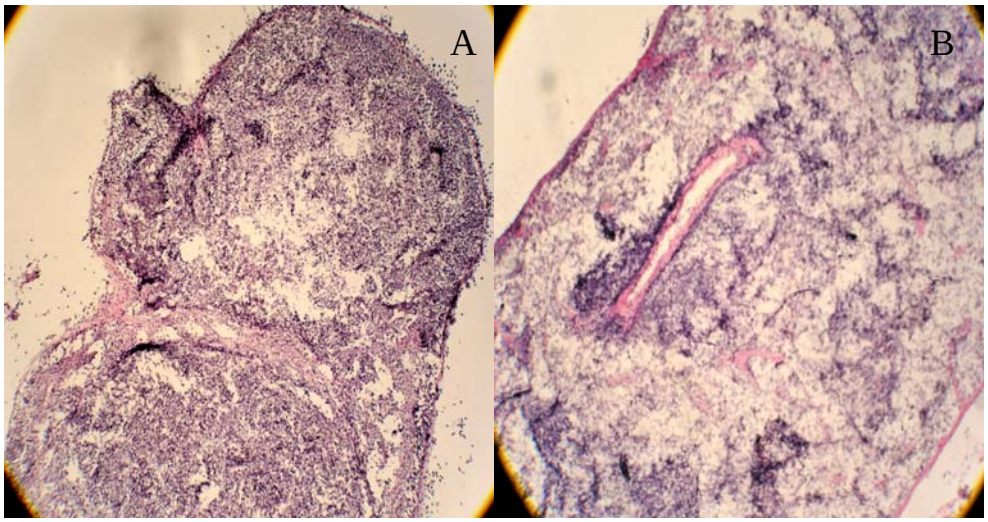

Figure 2. (A) H&E staining of a BALB/c Naïve lymph node under 4x magnification. The pink staining is the plasma membranes and connective tissue, and the purple staining is the nuclei of the cells. (B) H&E staining of a BALB/c Naïve spleen under 20x magnification. The pink oval appears to be a blood vessel.

II. Antibody Staining Optimization Experiments

To maximize fluorescence and minimize waste, several dilutions of the primary and secondary antibodies were tested: 1:250, 1:500, and 1:700. The dilution of 1:500 worked best for both the primary and secondary anti-Lyve-1 and anti-CD31 antibodies (data not shown). From these experiments it was deduced that the lymph nodes were easier to section and stain than the spleen, therefore the lymph nodes became the focus of

this study. Furthermore, different exposure times of the camera were tested during this experiment. The goal was to capture pictures of the sections that were representative of what was seen through the microscope. It was found that 5000 ms exposure time produced pictures that were comparable to what was viewed through the microscope; this exposure was used through out all the experiments (data not shown).

III. Protease Assay Optimization Experiments

The protease assay is a continuous reaction that can not be slowed or stopped once it has begun. The incubation time begins once the casein substrate is placed on top of the tissue section and the coverslip applied. Three incubation time points were tested: 1.5 hrs, 3 hrs, and 24 hrs to find the perfect balance between thorough staining and time efficiency (Figure 3). The best time for the incubation appeared to be 3 hrs since the 24 hr time point exhibited the same amount of staining. The 1.5 hr time point was incompletely stained, and it did not show the morphology clearly.

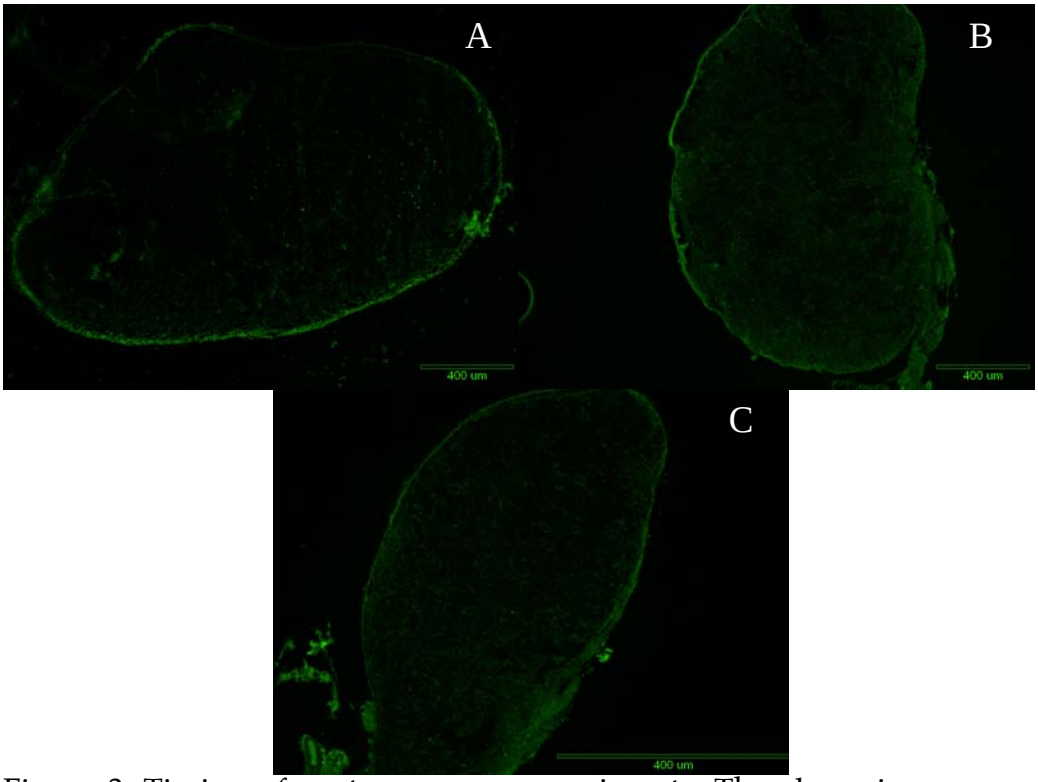

Figure 3. Timing of protease assay experiments. The above images were taken from BL/6 3 day MuLV infected mesenteric lymph nodes viewed at 4 x magnifications and incubated for (A) 1.5 hours, (B) 3 hours, and (C) 24 hours. (B.) 3 hours shows the best fluorescence that is comparable to 24 hours but more time efficient.

Once the incubation time was optimized, the next factor affecting the images is the exposure time of the camera. The longer the camera is exposed to the fluorescence the higher the recorded intensity level. Ideally, the pictures taken should be representative of what is seen when looking through the microscope. Three exposure times were tested: 1000ms, 3000ms, and 5000ms. In all cases, 1000ms was the best representative of the original microscope view (data not shown).

IV. Triple Staining

Triple staining with the protease assay, CD31 staining (red), and 4,6-diamidino-2-phenylindole (DAPI) staining (blue) was used to show protease localization around vascular structures along with individual cell nuclei (Table 5).

Table 5. Staining methods and purpose. The table below clarifies the structures that were stained and what was used to detect their presence.

Staining For:	Protease Activity Blood Vessels Nuclei
Using:	Casein substrate Anti-CD31 antibody staining DAPI staining

First, the tissue was stained with anti-CD31 antibodies, and then it was followed with the protease assay (Figure 4A). The second experiment stained the tissue with anti-CD31 and DAPI before beginning the protease assay (Figure 4B). Unfortunately, neither of these experiments worked as expected. The CD31 staining did not show the fluorescence seen in previous experiments, nor did it show blood vessel specificity. The DAPI staining hindered the visual identification of cell structures instead of enhancing the visualization of tissue morphology. The protease staining was unaffected and visually comparable to the previous stains when viewed alone. However, the *in situ* zymography procedure interfered with attempts to use other stains. Therefore, from this point forward, protease detection was conducted without the inclusion of other stains.

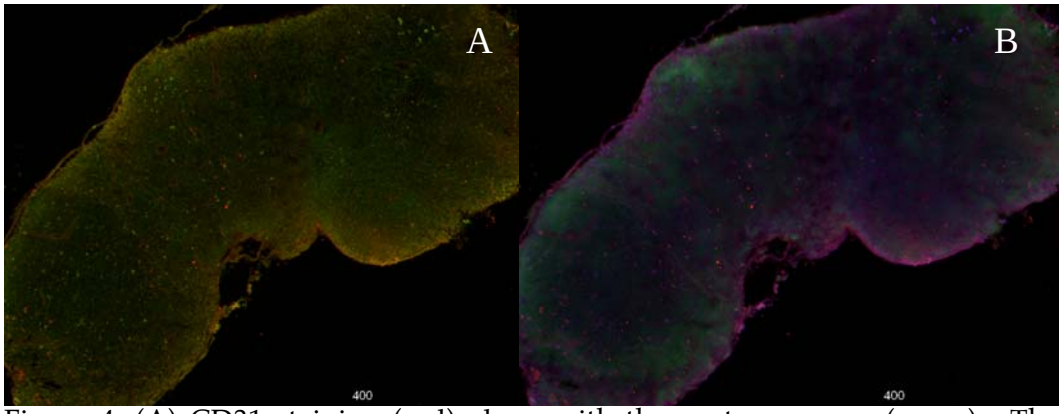

Figure 4. (A) CD31 staining (red) along with the protease assay (green). The yellow is the result of the overlapping of the CD31 and protease staining. The CD31 staining does not appear to be specific. (B) CD31 and DAPI (blue) staining along with the protease assay. The DAPI overshadows the other stains and the tissue morphology creating a blue hue.

V. Lymph node Tissue Staining

Fluorescent images were photographed using the Nikon Eclipse TE2000-U inverted fluorescence microscope and MetaVue software. Three different lymph nodes (mesenteric, axial/brachial combined, and inguinal) were stained for protease activity, lymphatic vessel location (Lyve-1), and blood vessel location (CD31). The mesenteric lymph nodes had the most pervasive and intense staining of all three types of lymph nodes (Figure 5 A-H). The green fluorescence identifies lymphatic vessels; these vessels are focused around the periphery and spread out into the cortex with a webbing pattern (Figure 5 A-D). The red fluorescence identifies blood vessels; these vessels are mostly seen as flat oval structures throughout the lymph node (Figure 5 A-D). The protease assay

did not show the localization that was expected and desired (Figure 5 E-H). Protease activity throughout the lymph node was observed with a few individual brighter patches.

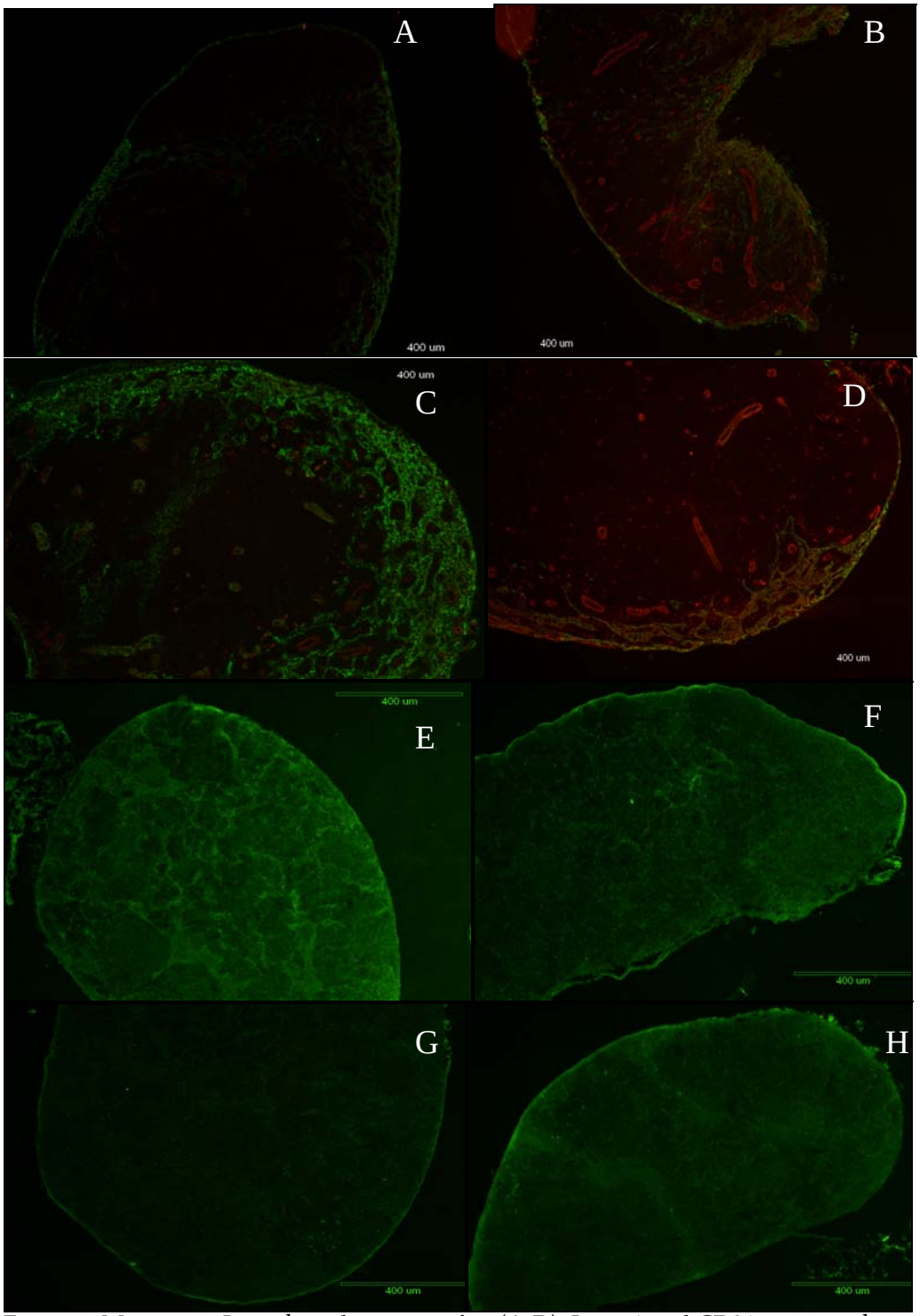

Figure 5. Mesenteric Lymph node staining for: (A-D). Lyve-1 and CD31 staining showing lymphatic (green) and blood vessels (red). (E-H.) Protease staining showing protease activity. (A, E) BALB/c MuLV infected mice. (B,F) BALB/c mock infected. (C,G) C57BL/6 MuLV infected mice. (D,H) C57BL/6 mock infected mice.

The inguinal lymph node stained well for Lyve-1 (green), but did not show the intensity of CD31 staining (red) that was seen in the mesenteric lymph node (Figure 6 A-D). There was also more red background staining in the inguinal lymph node, which is seen as an overall red haze throughout the lymph node. The protease staining was also mostly uniform across the lymph node regardless of the type of infection or strain of mice. The morphology and distinctive texture seen in the mesenteric staining is less apparent in the inguinal lymph node (Figure 6 E-H). The BALB/c strain appears to have more intense Lyve-1 and CD31 staining, along with higher blood vessel prevalence. This is especially apparent in the BALB/c mock infected sections. There is not a large difference between MuLV infected and mock infected mice in the Lyve-1 and CD31 staining, although the mock infected mice seem to have higher protease activity.

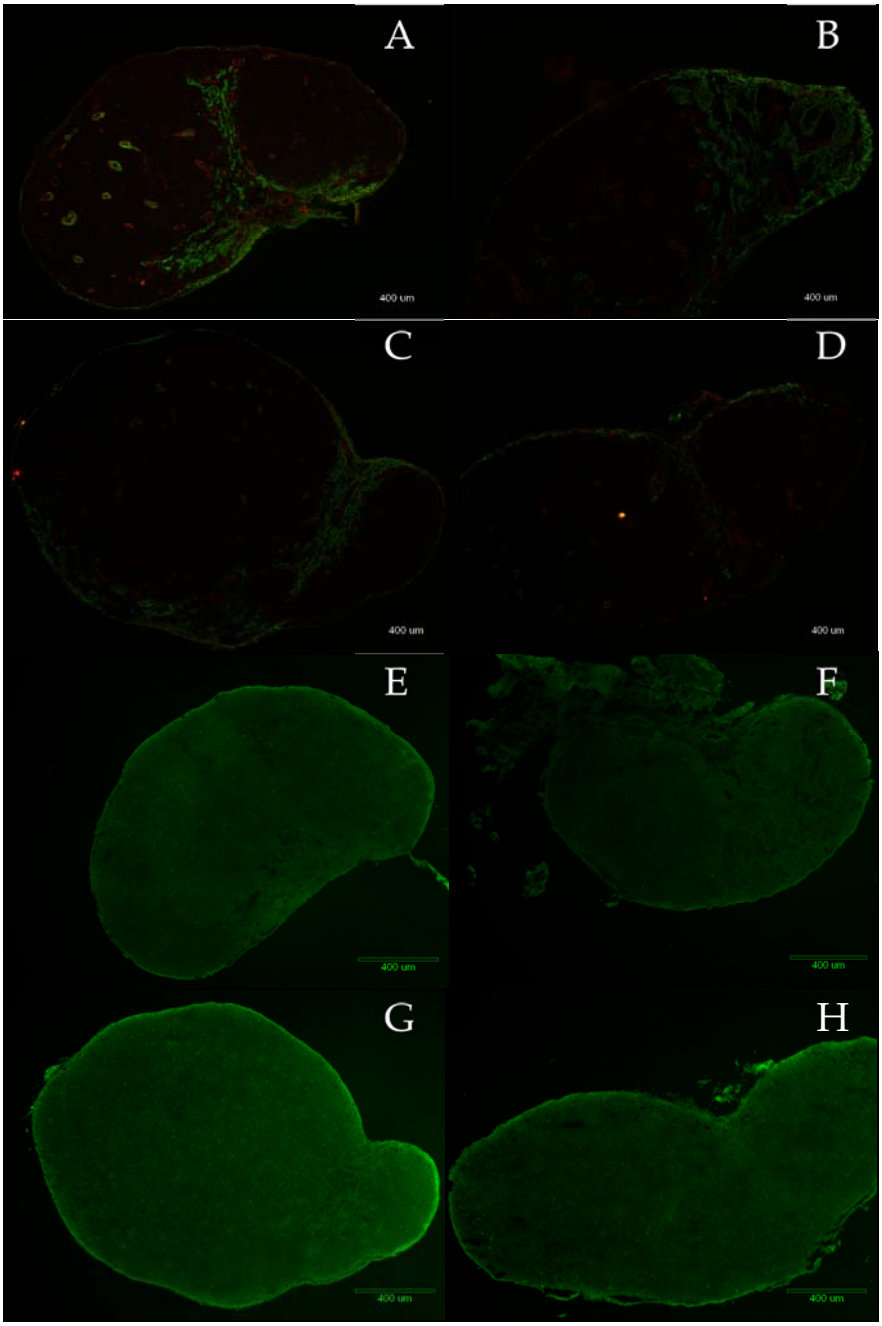

Figure 6. Inguinal Lymph node staining for: (A-D). Lyve-1 and CD31 staining showing lymphatic (green) and blood vessels (red). E-H. Protease staining showing protease activity (green). (A, E) BALB/c MuLV infected mice. (B,F) BALB/c mock infected. (C,G) C57BL/6 MuLV infected mice. (D,H) C57BL/6 mock infected mice.

Lastly, axillary/brachial lymph nodes were stained. Since the two lymph nodes are located so closely they were grouped together during the freezing process. They were comparable to the mesenteric lymph node staining except that they also had higher amounts of red background (Figure 7 A-D). In the axillary/brachial lymph nodes there seemed to be a greater number of large blood vessels that stretched across the lymph node. The protease staining in the axillary/brachial lymph node showed more tissue morphology than the inguinal lymph nodes, but it wasn't as detailed as the mesenteric lymph nodes (Figure 7 E-H).

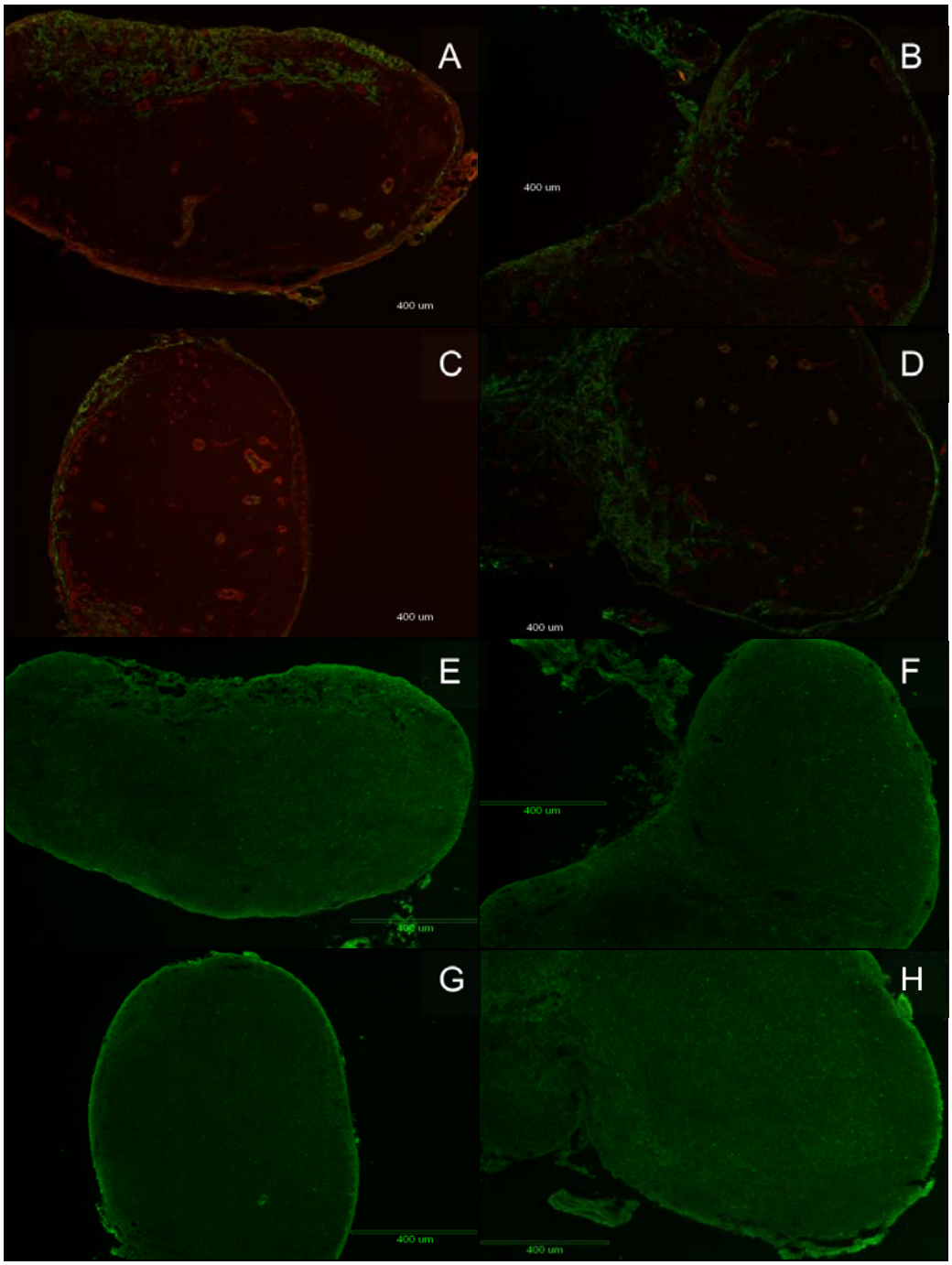

Figure 7. Axillary/Brachial Lymph node staining for: (A-D). Lyve-1 and CD31 staining showing lymphatic (green) and blood vessels (red). (E-H). Protease staining showing protease activity (green). (A, E) BALB/c MuLV infected mice. (B,F) BALB/c mock infected. (C,G) C57BL/6 MuLV infected mice. (D,H) C57BL/6 mock infected mice.

Overall, the mesenteric lymph node staining was the most consistent, with the most extensive vessel staining. The protease staining of the mesenteric showed the best tissue morphology of all the lymph nodes, and only the mesenteric lymph node showed an increase in staining from the mock infected to the MuLV infected. Since the mesenteric lymph node is the draining lymph node for our injection site, it may be the only lymph node fully responding to the infection.

VI. Protease Negative Control Experiments

The protease assay did not come with a standard negative control reagent, aside from not adding the substrate to the agar. In order to assess the level of non-specific fluorescence of uncleaved substrate, tissue autofluorescence, and non-specific enzymatic activity negative control experiments were conducted using inhibitor cocktails. Two types of inhibitors were used, a serine-protease specific inhibitor and a general protease inhibitor. The general protease inhibitor functioned to account for what is mentioned above. The serine protease specific inhibitor served to give insight on the amount of fluorescence due to serine specific proteases. The assay is similar to the blocking step in the immunofluorescence protocol, and was tried two different ways. The first attempt included a 1x TBS wash cycle, while the second attempt did not

include this step. Both trials showed complete fluorescence for both inhibitors (data not shown), and it appears that the inhibitors are not working properly. This experiment is still in progress.

VII. Lymph node Staining Patterns

To determine the overall trends in each mouse strain, the values of each individual lymph node staining were averaged to form one value for each strain and infection (Figure 8 and 9). There is not a clear pattern or trend with either stain. In the protease staining, the C57BL/6 mouse strain appears to increase slightly with infection, and the BALB/c mouse strain appears to decreases with infection. BALB/c mock infected mice have the highest protease activity (195.2), very closely followed by C57BL/6 MuLV infected mice (181.3), C57BL/6 mock infected mice (162.3), and BALB/c MuLV infected mice (162.3). All these values were in close proximity, and with only two biological replicates, calculations of statistical significance was not possible.

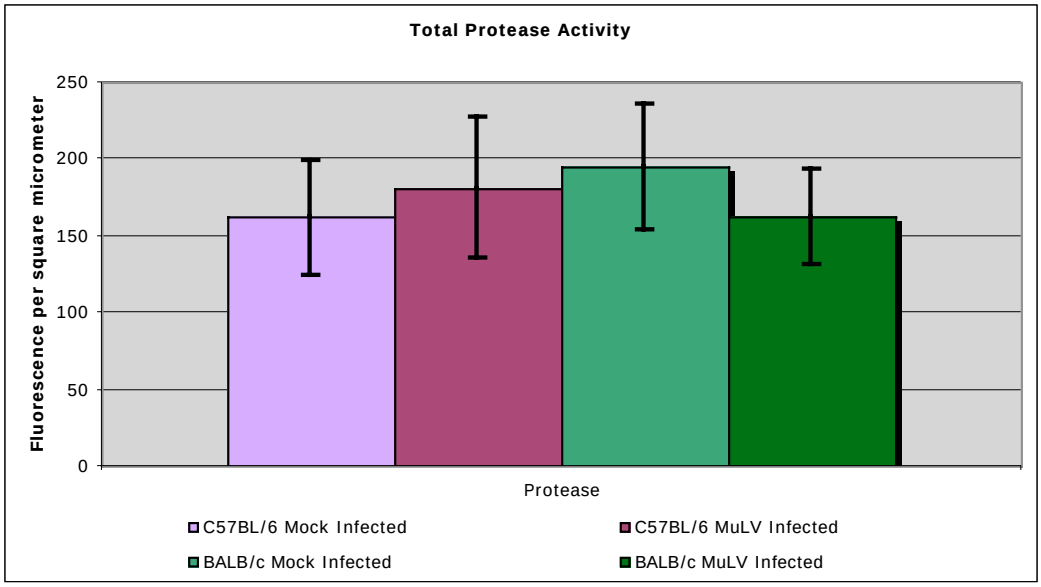

Figure 8. Total protease activity in each strain. This experiment averaged the data from all three types of lymph nodes, n = 2.

Similar to the protease activity, there is not a clear pattern in the Lyve-1 or CD31 staining (Figure 9). The Lyve-1 trend shows a slight increase in both strains with infection. The CD31 trend shows C57BL/6 mouse strain decrease with infection while the BALB/c mouse strain seems to increase with infection. BALB/c MuLV infected mice had the most staining for both Lyve-1 (13.9) and CD31 (11.2). In the CD31 staining, it is followed by C57BL/6 mock infected mice (9.6), C57BL/6 MuLV infected mice (8.6), and BALB/c mock infected mice (8.6). In the Lyve-1 staining, BALB/c MuLV infected mice (13.9) are followed by C57BL/6 MuLV infected mice (13.7), BALB/c mock infected mice (13.5), and C57BL/6 mock infected mice (12.6). All these values are within 2% of each other, and all the error bars overlap.

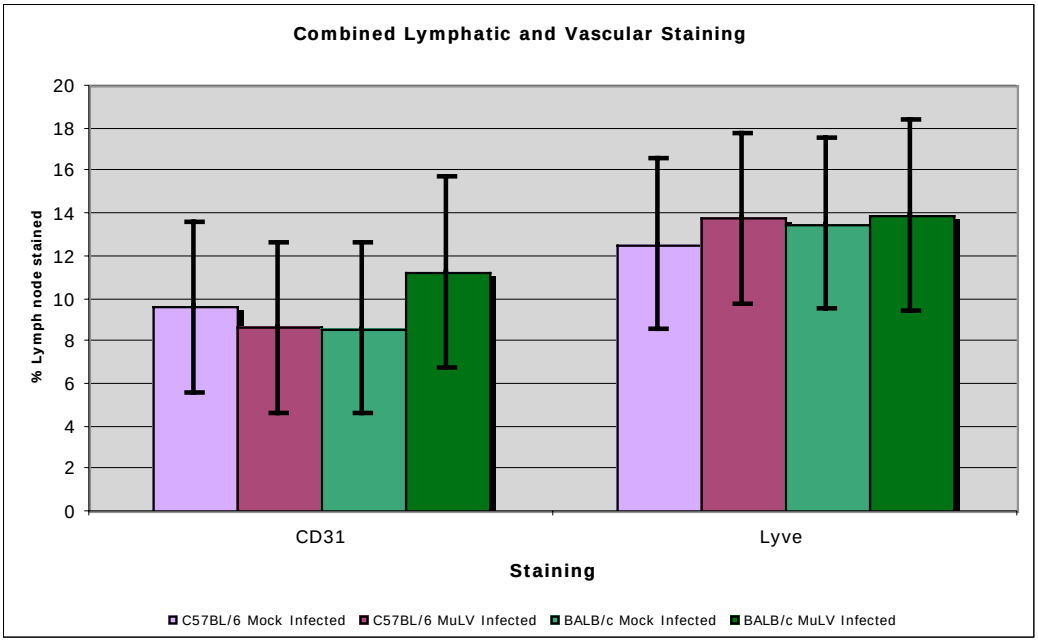

Figure 9. Lymphatic and blood vessel staining of each mouse strain in all three types of lymph nodes. The CD31 staining is on the left while the Lyve-1 staining is on the right. Standard deviation was calculated and n = 2.

VIII. Differences Between Types of Lymph nodes

A. Mesenteric Lymph node

The location of the lymph node is a factor in the experiment since its location will either decrease or extend the time it takes for the pathogen to reach it. Each lymph node was looked at individually to see regional trends. First, protease activity and the lymphatic/vascular staining was looked at in the mesenteric lymph node, the draining lymph node in relation to our injection site (Figure 10 & 11). The mesenteric lymph nodes

are located in the gut region of the mice inside the intraperitoneal cavity, where the virus is injected. The protease activity, as indicated below, was highest in the C57BL/6 MuLV infected mice (188.8) (Figure 10). This was closely followed by BALB/c mock infected (171.7), BALB/c MuLV infected (159.9), and C57BL/6 mock infected mice (149.6) in descending order.

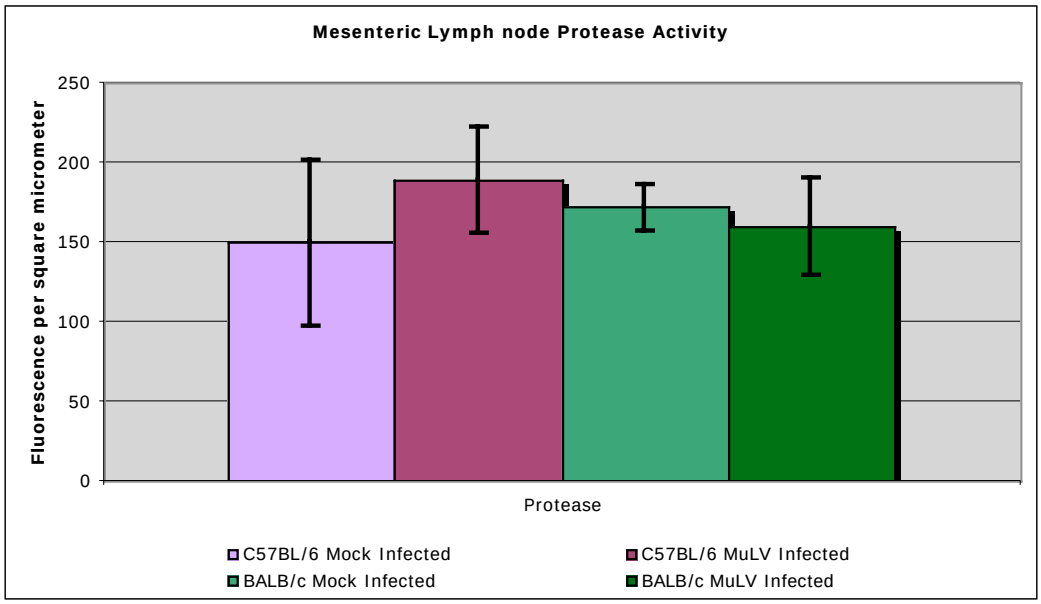

Figure 10. Mesenteric Lymph node protease activity for both mouse stains. The x-axis is the strains and infectivity and the y-axis is the fluorescence per square micrometer. Standard deviation was calculated using both biological replicates, n = 2.

The CD31 and Lyve-1 staining were both highest in the C57BL/6 MuLV infected mice (11.0 and 18.5 respectively) (Figure 11). In the CD31 staining, they were followed by BALB/c MuLV infected mice (9.7), C57BL/6 mock infected mice (8.9), and BALB/c mock infected mice (7.8).

In the Lyve-1 staining BALB/c MuLV infected (16.1) and mock infected mice (16.0) have about the same amount of Lyve-1 staining, and they are followed by C57BL/6 mock infected (12.0) with the least amount staining.

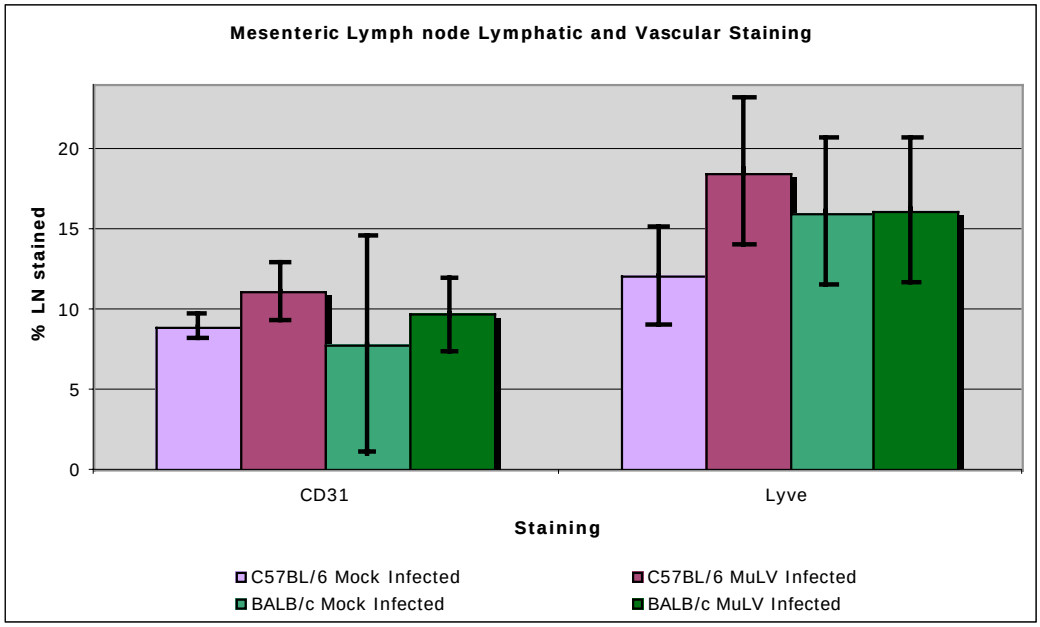

Figure 11. Mesenteric Lymph node lymphatic and blood vessel staining. The x-axis is the strains and infectivity and the y-axis is the percent of the lymph node covered with the stain. Standard deviation was calculated using both biological replicates, n = 2.

The amount of protease activity correlates with the Lyve-1 and CD31 staining in the mesenteric lymph node (Figures 12 and 13). When the graphs are overlaid, the correlation is easily seen, both the CD31 staining and protease activity overlay (Figure 12) and the Lyve-1 and protease activity overlay (Figure 13) show a trend of C57BL/6 MuLV infected mice as having the most protease activity and the highest percentage of vessel coverage.

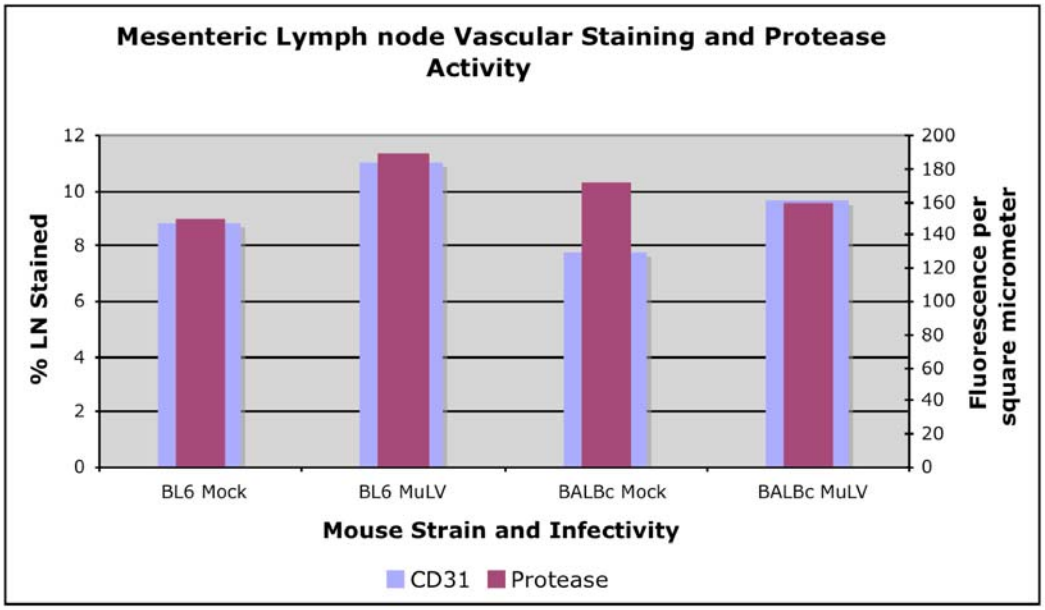

Figure 12. Overlay of the protease activity graph and the CD31 staining graph. The two stains show the same trends, C57BL/6 MuLV infected mice have the highest protease activity and the most CD31 staining.

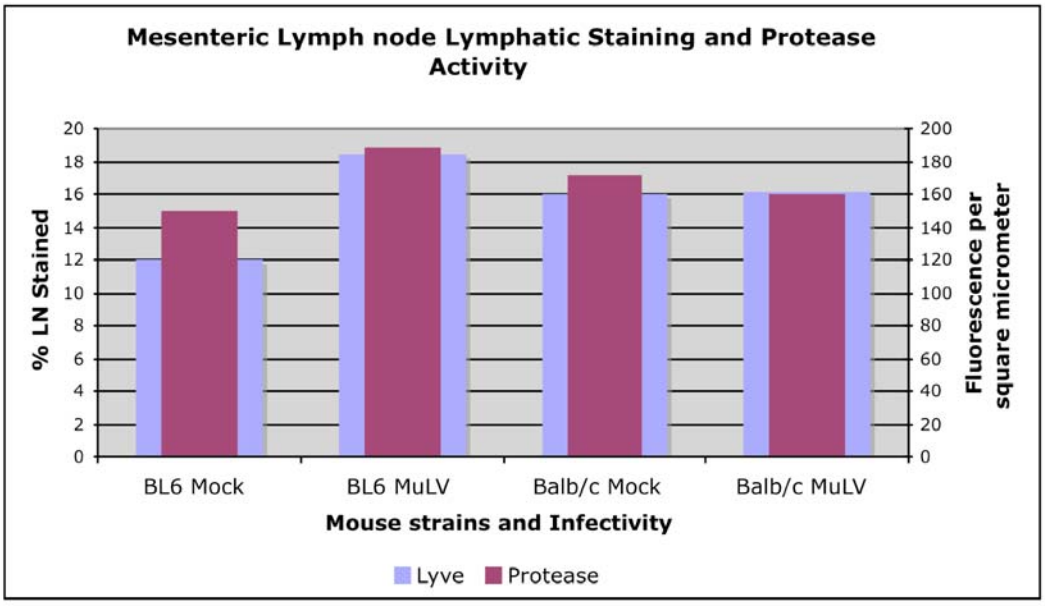

Figure 13. Overlay graphs of protease activity and Lyve-1 staining. The two stains show the same trends, C57BL/6 MuLV infected mice have the highest protease activity and the most Lyve-1 staining.

B. Inguinal Lymph node

The next set of lymph nodes tested were the inguinal lymph nodes located in the subcutaneous tissue of the groin (Figures 14 and 15). The only trend present is the apparent decrease in all the stains after infection in both strains. BALB/c CD31 staining is the one exception (Figure 15). BALB/c mock infected mice (184.2) had the greatest amount of protease activity (Figure 14). This was followed by BALB/c MuLV infected mice (158.7) and C57BL/6 Mock infected mice (157.1) with about the same amount of activity, and C57BL/6 MuLV infected mice (138.9) with the lowest amount of activity. All these values were within 50 square micrometers of each other, and all the error bars are overlapping.

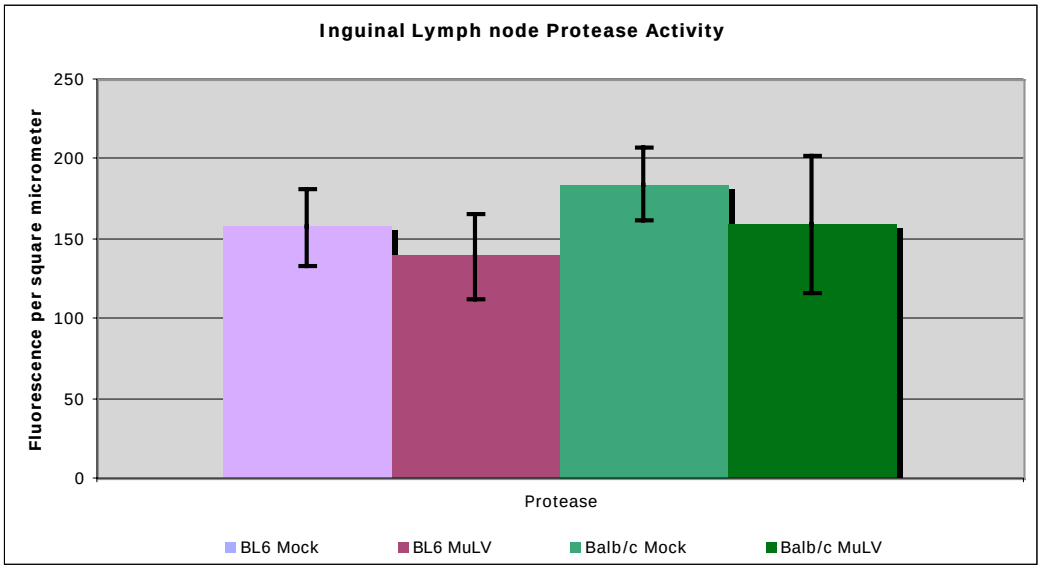

Figure 14. Protease activity for inguinal lymph nodes. The x-axis is the strains and infectivity and the y-axis is the fluorescence per square micrometer. Standard deviation was calculated using both biological replicates, n = 2.

For both Lyve-1 and CD31, C57BL/6 Mock infected mice have approximately 2% more staining with both Lyve-1 and CD31 staining than the other samples tested (13.8 and 11.2 respectively; Figure 15). For the CD31 staining, the other three samples were within 1% of each other. C57BL/6 MuLV infected mice (9.7%) were the second highest, with BALB/c MuLV infected mice (9.1%) and BALB/c mock infected mice next (8.7%). For the Lyve-1 staining, the others were within 1% of each other. BALB/c mock infected mice (12.0%) being the second highest, and C57BL/6 MuLV infected mice (10.6%) having about the same amount as BALB/c MuLV infected mice (10.4%).

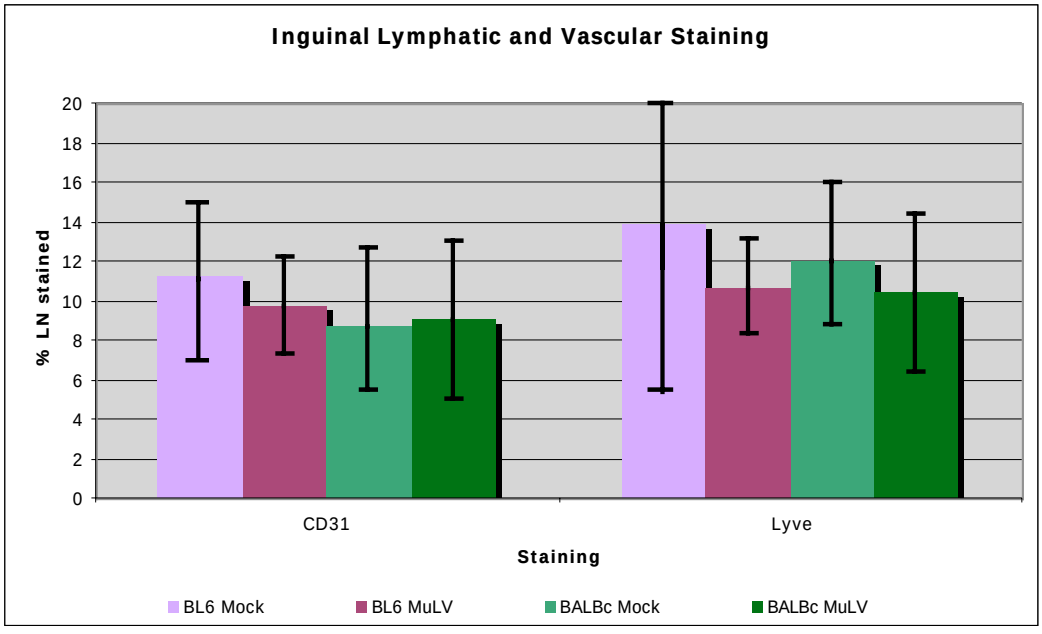

Figure 15. Lymphatic and blood vessel staining for inguinal lymph nodes. The x-axis is the strains and infectivity and the y-axis is the percent of the lymph node covered in staining. Standard deviation was calculated using both biological replicates, n = 2.

C. Axillary and Brachial Lymph nodes Combined

The final group of lymph nodes looked at was the axillary and the brachial lymph nodes located under the tricep and in the armpit. These two types of lymph nodes were grouped together because of their close proximity. For this protease experiment (Figure 16), the BALB/c mock infected mice had the most staining (229.7), C57BL/6 MuLV infected mice (205.4) have the second highest followed by BALB/c MuLV infected mice (174.5) and C57BL/6 mock infected mice (140.7). All the values are within 100 square micrometers of each other.

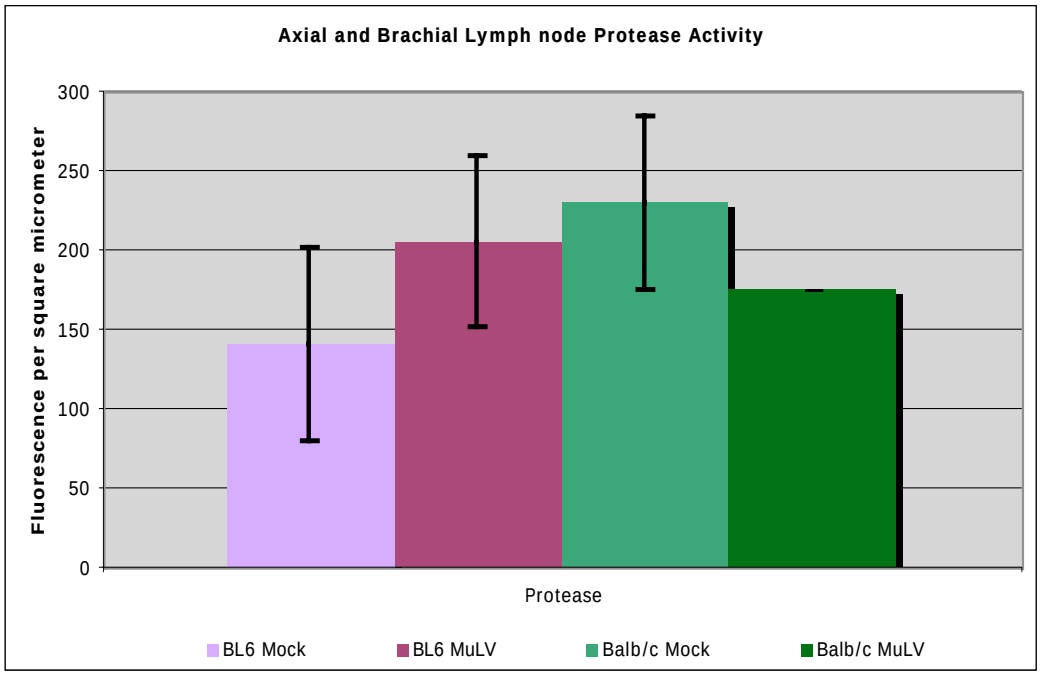

Figure 16. Axillary and Brachial lymph node protease activity in all mouse strains and infectivities. The x-axis is the strains and infectivity and the y-axis is the fluorescence per square micrometer. Standard deviation was calculated using both biological replicates, n = 2.

The Lyve-1 and CD31 staining in the axillary and brachial lymph nodes (Figure 17) did not correlate with the protease activity; BALB/c MuLV infected mice (17.7 %) were higher than all others in the CD31 staining and slightly higher than the rest in the Lyve-1 staining (16.5%) (Figure 17). In the CD31 staining, this is followed by BALB/c mock infected mice (9.2%), C57BL/6 mock infected mice (8.5%), and C57BL/6 MuLV infected mice (7.6%), all these values are within 1% of each other. In the Lyve-1 staining, BALB/c MuLV infected mice (16.5%) are followed by BALB/c mock infected mice (12.5%), C57BL/6 MuLV infected mice (12.0%), and C57BL/6 mock infected mice (11.4%). The Lyve-1 staining showed the trend expected to be seeing in all the lymph nodes, but again, all these values are within 1-4% of each.

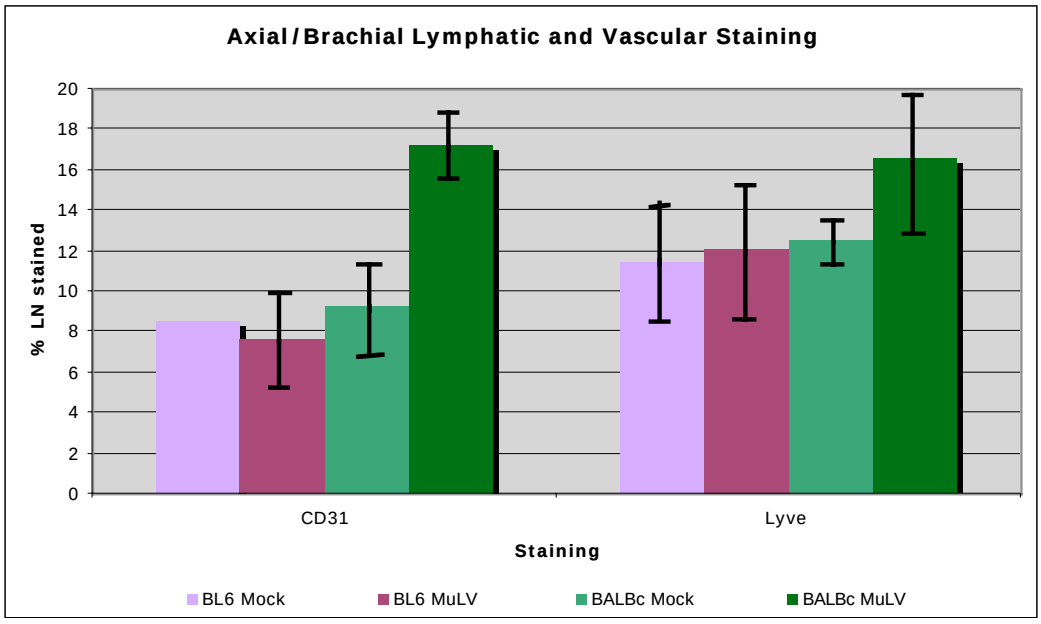

Figure 17. Axillary/Brachial lymph node lymphatic and blood vessel staining. The x-axis is the strains and infectivity and the y-axis is the percent of the lymph node covered in staining. Standard deviation was calculated using both biological replicates, n = 2 for all except BL/6 mock infected where n=1.

The mesenteric lymph node staining was the most consistent, and showed a clear correlation between protease activity and vessel prevalence. Although the trends were variable, overall C57BL/6 MuLV has the highest protease activity and the most lymphatic and blood vessel coverage. The protease staining of the mesenteric showed the best tissue morphology of all the lymph nodes, and only the mesenteric lymph node showed a consistent increase in staining from the mock infected to the MuLV infected.

DISCUSSION

Proteases are essential for a variety of biological processes throughout the body. This research has shed some light on a new method of looking at protease activity, *In situ* zymography. *In situ* zymography has the potential to explore enzyme activity from a new angle. It illuminates the differences between gene activity, protein translation, and enzyme activity. Using this new technique allows for a comparison between the two mouse strains, and follows up on the microarray work previously done.

This research uses the murine leukemia virus (MuLV) mouse model system to study AIDS. This model system utilizes two mouse strains, BALB/c and C57BL/6. Both strains become infected, but while the BALB/c mouse strain will recover, the C57BL/6 mouse strain becomes immune compromised. This research compares protease activity at the protein level in the lymph nodes of each mouse strain 3 days post infection. It is already known that lymphatic remolding and cell activation are consequences of protease activity (Sun and Zhang, 2006), and an increase in lymphatic vessels allows for an increase in immune cell circulation, activation, and control of an infection. I have proposed that the upregulation of these proteases will cause lymphatic remolding contributing to the recovery of the BALB/c mouse strain.

I. *In situ* Zymography

The first goal of this research was to create and optimize a protocol for *in situ* zymography, and ultimately combine this with immunofluorescence staining. This technique is a relatively new procedure in the field and a full protocol wasn't available. A protocol was compiled using various resources and optimized by experimenting with a variety of parameters. There were three main parts to the assay: (1) tissue preparation and freezing, (2) sectioning, and (3) staining and analysis.

The most variable and temperamental part of the experiment was the tissue freezing. Slight variations in tissue extraction methods and freezing time resulted in tissues that were unable to be sectioned. During the tissue extraction, if any significant pressure was applied to the whole organ the membrane would be ruptured and the sections would not remain whole. After the tissue was extracted if it was not immediately frozen or if it was not frozen quickly enough then it resulted in different tissue texture. Occasionally this would result in a crystallization of the tissue, rendering it unable to be sectioned without crumbling.

Sectioning the tissue was long and tedious but did not add the same amount of variability to the experiment because if the section was not up to the standards set prior to beginning the experiment it could not be used. The biggest problem faced while sectioning was tissue disruption, and the only solution is continual technique improvement.

A. Triple Staining

Initially the protease assay was combined with the CD31 immunofluorescent staining and DAPI nuclei staining. The tissue was first stained for CD31, which was followed by the protease assay with DAPI added to the agar afterwards (Figure 4A,B). Unfortunately, this was not successful. The CD31 staining lost all specificity and instead only showed up as nonspecific spots appearing to be more background than actual staining. This may be due to an interference with the secondary antibody and the agar, causing a lower binding affinity to the primary antibody and leading to detachment. Also, it seemed that the agar used for the protease assay caused low levels of red fluorescence on its own; this was seen in the negative controls. Interestingly, the CD31 staining had no effect on the protease assay, which was the original concern. The DAPI staining bled into all of the tissue, creating a bluish white hue over the whole section. It did not show the specific nuclei as desired and only interfered with the other stains. Instead of combining the staining, serial sections were stained with CD31 and for protease activity. If necessary, the photos could then be overlain to show localizations.

B. Protease Assay Staining Characteristics

The protease assay did not show the localized staining pattern that was anticipated. Instead, there was a global staining with some areas of increased intensity. This made it difficult to show any localized fluorescence relative to vessel formation, or even vessel presence. It was more accurate to compare the area of the lymph node covered by vascular and lymphatic vessels to the overall protease staining intensity.

The slides were visualized on an inverted fluorescent microscope and analyzed with MetaVue software. This allowed the pictures to be taken the day of the staining and analyzed using the same software on another day. For the protease staining, the intensity per square micrometer was measured. This allowed correction for the varying lymph node sizes, and averages between mouse strains, lymph nodes, and types of infections were compared.

C. Inhibitors

The protease assay is relatively new and did not come with a negative control, besides using the agar devoid of the substrate. To ensure the assay was specific, inhibitors were incorporated to act as negative controls. There were two sets of inhibitors used, an overall protease

inhibitors and a specific serine protease inhibitor. This would show if the cleavage was specific to proteases only, and it would show if serine proteases were a significant part of the active enzymes detected. Unfortunately, the inhibitors also did not come with a protocol. One was compiled based on the blocking step in the immunofluorescent staining. When the formulated procedure was first attempted, the mistake of rinsing the slide with 1x TBS after incubation with the inhibitors was made. The inhibitors were probably washed off the section, which is why they were not effective, and full fluorescence was seen. The second attempt of the procedure did not include the washing step, instead the slide was drained of the excess inhibitors after the incubation. Immediately after the protease agar containing the casein substrate was applied. Again, the inhibitors were not effective and full fluorescence was seen. Prof. Lilian Hsu was consulted about the assay, and she suggested testing different concentrations of the inhibitors. This aspect of this project is still underway.

II. Immunofluorescence

The immunofluorescent staining also utilized the same tissue preparation as the *in situ* zymography. Since serial sections were used, the same organs were used and the same overall tissue and sectioning process

was used. Before the staining could begin, different dilutions of the primary and secondary antibodies for Lyve-1 and CD31 needed to be tested. Three dilutions of each were tested: 1:250, 1:500, and 1:700. The dilution 1:500 for the primary and secondary of both antibody sets showed the most thorough staining with the least amount of background.

The staining overall was successful. The CD31 staining was the most difficult, because the wavelength that was used to view red fluorescence would also brightly illuminate most other foreign particles in the section, such as dust, bubbles, etc. If the particle's fluorescence could not be removed using the upper threshold limits than the section could not be used.

Since the amount of vasculature present in each lymph node is being studied, the intensity of the fluorescence is not as important as the area it covers. Therefore, instead of measuring intensity per square micrometer, the percentage of the lymph node area covered in lymphatic and blood vessels were measured. This way the amount of vessels per lymph node in relation to its size could be compared. This will account for varying organ size and section size.

III. Combined Lymph node Staining

As it was stated in the results, there was no clear pattern between the combined lymph node immunofluorescence staining and the protease staining. The BALB/c 3 day mock infected mouse strain had the highest amount of protease activity while the BALB/c 3 day MuLV infected mouse strain had the greatest area covered by lymphatic and blood vessels. However, these results are not believed to reflect the mouse's response to the infection. It is possible that each lymph node is reacting differently depending on its location. Since the mesenteric lymph node is the closest to the injection site, and is most likely the draining lymph node for the area, it may more accurately display the immune response towards MuLV infection. Furthermore, since there are only two biological replicates and two experimental replicates per strain and infection type, statistical significance in unable to be drawn from the data.

III. Individual Lymph node Stains

A. Mesenteric Lymph node Staining

Although all the lymph nodes have been tested, due to the mesenteric lymph node's location and key role in the draining of the

injection site, the patterns seen here are the most interesting (Figures 10 and 11). The protease activity (Figure 10) was the highest in the C57BL/6 MuLV infected mice, and the most lymphatic and blood vessels (Figure 11) were also seen in the C57BL/6 MuLV infected mice. This was surprising, since it is exactly opposite from what was expected and what the microarray data suggested at the mRNA level. This implies that there may be a large discrepancy between what is being transcribed and translated. Therefore, genetically there may be an upregulation in protease gene expression, these mRNAs may not be translated into protein or the proteases are not activated in vivo.

There are numerous reasons for this difference in expression. A large possibility is that this experiment tests for active proteases, not the presence of pro-enzymes. Proteases are commonly stored in cells and tissues with endogenous inhibitors, waiting for the appropriate signal to be released. These proteases will not be revealed in this assay, and their presence will not be detected. Another possibility is that protease gene expression is upregulated three days post infection, but upregulation of active proteases is further out, maybe five or six days post infection. Finally, there could be a problem with the assay not being specific enough. If the specific proteases that the microarray data suggested were upregulated were tested for, then a difference may be seen. Instead the assay is broad, and there maybe such a large number and variety of proteases present in the lymph node normally that causes these individual

difference in a few enzymes to be masked. These possibilities and more will be discussed later.

B. Axillary and Brachial Lymph node Staining

The results of the axillary and brachial staining did not show a significant pattern (Figure 16 and 17). The BALB/c mock infected mice had the highest amount of protease activity, while BALB/c MuLV infected mice had the most lymphatic and blood vessels. All these values were very close to each other with large differences within replicates and without statistical significance. The Lyve-1 staining showed the trend I expected to see in all the lymph nodes, but again, all these values are within 1% of each other. The BALB/c MuLV infected mice are the exception.

C. Inguinal Lymph node Staining

The inguinal lymph node was the hardest to extract without causing damage to the tissue, and was therefore the hardest to section uniformly. These difficulties led to imperfect sections and tissue interference within the section, i.e. tissue folding, wrinkling, or disruption.

These imperfections did not significantly effect the staining, but since this is not a draining lymph node this lymph node should be used for further testing. The difficulties in extraction and the tissue damage may change the natural protease expression and activity leading to false results.

There was no clear pattern in the protease staining (Figure 14); BALB/c mock infected mice had slightly more protease activity than the rest. All these values were within 50 square micrometers of each other with overlapping error bars, so again the statistical significance is not present. For both Lyve-1 and CD31 staining (Figure 15), C57BL/6 mock infected mice had the highest vessel coverage by 2%.

IV. Microarray Data versus Protein Activity Data

To conclude the results, I have found that there is no overall pattern in the combined lymph node staining, and a correlation between protease activity and vessel growth could not be made. Of the three lymph nodes, the mesenteric lymph node seems to be the most accurate in response to the injection, and the most important since it may be the draining lymph node for our injection site. The mesenteric lymph node did show a relationship between protease activity and vessel growth, although it was contradictory to what was hypothesized and what the microarray data suggested at the mRNA level. It suggested that protease activity was

higher and lymphatic and blood vessels covered a larger percent of the C57BL/6 MuLV infected mouse strain.

The next logical question is why my data does not support the microarray data? As it was previously stated, it could be a difference in what is being transcribed and translated. There is not a one to one relationship of mRNA transcription and protein translation. Also, there are a number of natural regulators of protease activity. These regulators serve to inhibit protease activity at the protein level until they are needed (Sun and Zhang, 2006). An example would be endogenous inhibitors; they bind to proteases to inactivate them (Boonacker et al, 2001). Even though these proteases are present at the protein level, they are kept inactive and waiting until the proper signal is given for their activation. Along with inhibitors, many proteases also need posttranslational activation, and can remain in the tissue and in cells in their inactive form (Boonacker et al, 2001). During posttranslational activation other proteases or enzymes will activate the protease by cleaving it. Many times this is a step within a signal cascade.

Another factor to be examined when comparing microarray data to protein expression is the possibility of lag time between the upregulation at the genetic level and the upregulation at the protein level. The activation of the genes encoding proteases are upregulated 3 days post infection. This does not mean that the protein expression will also be present at 3 days post infection. A small amount of time could be present

between genetic expression and protein expression, therefore testing other days would be important for future work.

The endogenous background protease activity needs to be further investigated as well. As was discussed earlier, if the background protease activity is considerably high, and the individual genes that are upregulated are naturally low when not responding to an infection, then when the upregulated genes increase their production it may only reach the background level of endogenous protease activity. This means that the assay will not detect a large change in activity when testing for global protease activity since the background activity will cause the majority of the fluorescence that is seen. Because a large difference between mock infected and MuLV infected sections is not seen, this could be a contributing factor.

Tissue treatment is another factor that may cause a discrepancy between the microarray data and the protease activity data. Careful technique is used to minimize this factor, but even so the death of the animal may cause immediate changes in the protease activity. The extraction process is another point that can cause damage to the tissue and may activate or inactivate proteases. Finally, the sectioning and freezing may have adverse affects on the proteases within the tissue. All of these small changes can cause a disruption in the overall trend that is being studied. As it was stated before, careful, consistent technique can circumvent most problems, but this should also be tested in the future.

This can be done by using a variety of assays to test for the protease activity and comparing the results to those recorded using *in situ* zymography.

Finally, the last factor is assay specificity. Since the protease assay did not come with a negative control reagent, aside from the agar alone, there is a possibility that the casein substrate is not specific enough and is being cleaved by other enzymes. To test this, a protocol was created using inhibitors, but they have not been functioning properly. This could be a result of the inhibitor concentration, or this could mean that my assay is not specific to proteases alone. Since not even a slight decrease is seen in fluorescence when using inhibitors, which would be expected even if the assay was not specific, it is not believed that the inhibitors are functioning properly. Further optimization is needed on the protocol and the inhibitor concentrations.

V. Conclusions

From these experiments it has been ascertained that protease activity is a difficult and elusive phenomenon to study. Further optimization and experimental replication needs to be done using *in situ* zymography to show the connection between protease activity and vessel growth. Although a trend towards correlation was seen in the mesenteric

lymph node staining, more biological replicates need to be performed to gain statistical significance and to show localization of specific protease activity. Also, more experiments would solidify the results showing that the C57BL/6 3 day MuLV infected mice have higher protease activity and more vessel coverage than the BALB/c 3 day MuLV infected mice. It is already known that the C57BL/6 mouse strain's peak cytokine and immune response to MuLV is delayed compared to the BALB/c mouse strain. Later, there are strong cytokine and non-specific immune responses. This overexpression causes more harm then good, and it would be interesting to examine if there is a connection between this escalated nonspecific immune response and an increase in protease activity. An increase in protease activity would cause an increase in lymphatic and blood vessel growth, which would further worsen the systemic overload.

Much work is needed to be done to perfect the technique of *in situ* zymography. However, these experiments have begun to shed light on the active protease levels in the two mouse strains, and to suggest patterns further confirming the relation between protease activity and lympho- and angiogenesis. To continue this research, optimizing the negative controls and showing assay specificity would be necessary. Ideally, testing other post infection time points is needed to show that the protein expression peak coincides with the genetic upregulation 3 days post infection. Also, using other assays to show the same results that were

obtained using *in situ* zymography would strengthen the results of higher protease activity in C57BL/6 infected mice. Further specific testing of individual proteases, such as serine proteases or elastases, specifically, can deviate from the problem of endogenous nonspecific protease activity. This would also show individual gene expression, its specific protein expression, and a ratio of mRNA production to active protein formation could be deduced. Finally, as with most scientific pursuits, increasing the number of experimental and biological replicates would greatly improve the result's validity and capacity of achieving statistical significance.

The relationship between protease activity and vessel growth is important in HIV research. If there is a correlation between the immune system's increased ability to fight off infection and protease activity, than this could be used for future therapy. Protease inhibitors are already being tested for pain therapy and prevention and are currently being used for treating HIV infections. HIV protease inhibitors prevent the cleavage of gag and gag-pol protein precursors, which is usually performed by HIV proteases (Flexner, 1998). These inhibitors prevent this cleavage in acutely and chronically infected cells. This stops maturation and blocks the infectivity of newly produced virons stopping subsequent waves of infection, although it does not clear cells that are already infected. These inhibitors are only effective in HIV type 1 and 2 (Flexner, 1998).

Once the signal pathways are better known, scientists may be able to induce a cascade to increase or decrease protease activity, which would

change lymphatic and blood vessel growth, ideally helping the body keep a low viral load or clearing the virus altogether. Any and all advances in research for a cure or a way to increase an HIV positive person's asymptomatic lifespan are desperately needed. Hopefully this research is the beginning of increased awareness of proteases' possible therapeutics for treating HIV infections.

REFERENCES

Boonacker E., Van Noorden C.J.F. "Enzyme Cytochemical Techniques for Metabolic Mapping in Living Cells, with Special Reference to Proteolysis." *Journal of Histochemistry and Cytochemistry.* 2001. **49(12).** 1473-1486.

Chattopadhyay S.K., Sengupta D.N., Frederickson T.N., Morse C.H.III,. and Hartley J.W. "Characteristics and Contributions of Defective, Ectotropic, and Mink Cell Focus-Inducing Viruses Involved in a Retrovirus-Induced Immunodeficiency Syndrome of Mice." *Journal of Virology.* 1991.**65**, 4232-4241.

Cirino1 G., Vergnolle N. "Proteinase-activated receptors (PARs): crossroads between innate immunity and coagulation" *Pharmacology* 2006, (6)428–434

Coffin J.M. "Structure, Replication, and Recombination of Retrovirus Genomes: Some Unifying Hypotheses" *Journal of gen.Virology.* 1979, **42** I-26

Deguchi J., Aikawa M., Tung C., Aikawa E., Kim D., Ntziachristos V., Weissleder R., Libby P. " Inflamaation in Atherosclerosis Visualizing Matrix Metalloproteinase Action in Macrophages In Vivo." *Circulation.* 2006. **114.** 55-62.

Flexner C. "Review: HIV-protease inhibitors". *New England Journal of Medicine.* 1998, 338(18) : 1281-92

Frederiks W., Mook O.R.F. "Metabolic Mapping of Proteinase Activity with Emphasis on In Situ Zymography of Gelatinases: Review and Protocols." *Journal of Histochemistry and Cytochemistry*. 2004. **52(6)**. 771-722.

Green, W.R., Crassi, K.M., Schwarz, D.A. and Green, K.A. "Cytotoxic T Lymphocytes Directed against MAIDS-Associated Tumors and Cells from Mice Infected by LP-BM5 MAIDS defective Retrovirus". *Virology.*1994. **200**. 292-296.

Janeway CA, Travers P, Walport M, Shlomchik MJ. 2001. Immunobiology 5th ed, Garland Publishing, New York.

Hartley, J.W., T.N Frederickson, R.A Yetter, M. Makimo and H.C Morse III. "Retrovirus-induced acquired immunodeficiency syndrome: natural history of infection and differing susceptibility of inbred mouse strains." *Journal of Virology*. **63.** 1223-1231.

Kim W.K., Tang Y., Kenny J.J., Longo D.L., Morse III H.C. " In Murine AIDS, B-cells are Early Targets of Defective Virus and Are Required for Efficient Infection and Expression of Defective Virus in T Cells and Macrophages" *Journal of Virology*. 1994, 6767-6769

Lee S., Tsuji K., Lee S., and Lo E. " Role of Matrix Metalloproteinases in Delayed Neuronal Damage after Transient Global Cerebral Ischemia" *Journal of Neuroscience.* January 1, 2004. **24(3).** 671-678.

Liang B., Wang J.Y., Watson R.R. "Murine AIDS, a Key to Understanding Retrovirus-Induced Immunodeficiency" *Viral Immunology* 1996, **9(4)** 225-239.

Liekens S, De Clercq E., Neyts J. "Angiogenesis: regulators and clinical applications" *Biochemical Pharmacology*. 2001 (61)253–270

Morse III H., Chattopadhyaya S.K., Makino M., Fredrickson T.N., Hugin A.W., Hartley J.W. "Retrovirus-induced immunodeficiency in the mouse: MAIDS as a model for AIDS" *AIDS* 1992, **6(7)** 607-621Murphy G., Gavrilovic J. " Proteolysis and cell migration: creating a path?" *Cell Biology 1999, **11**:614-621*

Ossovskaya V.S., Bunnett N.W. "Protease-Activated Receptors: Contribution to Physiology and Disease". *Physiol Rev.* 2004 84: 579–621

Rowland-Jones, S.L. and McMichael, A. "Immune Responses in HIV-exposed seronegatives: have they repelled the virus?" *Current Opinion in Immunology*. 1995. **7,** 448-455.

Saban R., D'Andrea M.R., Andrade-Gordon P., Derian C.K., Dozmorov I., Ihnat M.A., Hurst R.E., Simpson C., Saban M.R. "Regulatory network of inflammation downstream of proteinase-activated receptors" *Physiology* 2007, **7**:3 1472-6793-7-3

Schmid-Schonbein, G. W. 2006. Analysis of Inflammation. Annu Rev Biomed Eng.

Skurnick, J.H, Palumbo, P., DeVico, A., Shacklett, B.L., Valentine, F.T., Merges, M., Kamin-Lewis, R., Mestecky, J., Denny, T., Lewis, G.K, Lloyd, J., Praschunus, R., Baker, A., Nixon, D.F., Stranford, S.,

Gallo, R., Vermund, S.H. and Louria, D.B. "Correlates of Nontransmission in US Women at High Risk of Human Immunodeficiency Virus Type I Infection through Sexual Exposure." *The Journal of Infectious Diseases*. 2002. **185**: 428-438.

Steinhoff, M., J. Buddenkotte, V. Shpacovitch, A. Rattenholl, C. Moormann, N. Vergnolle, T. A. Luger, and M. D. Hollenberg. 2005. Proteinase-activated receptors: transducers of proteinase-mediated signaling in inflammation and immune response. Endocr Rev 26:1-43.

Sun X., Zhang H. "Clinicopathological significance of stromal variables: angiogenesis, lymphangiogenesis, inflammatory infiltration, MMP and PINCH in colorectal carcinomas" *Molecular Cancer* 2006, 5(43)1476-4598

Tepsuporn, Suprawee. 2005. Mount Holyoke College Thesis

Topor Y., Magne-Watts B., Barton-Knott S., Nandra I. "Global AIDS epidemic continues to grow" *World Health Organization and United Nations AIDS Council.* accessed 2006. http://www.who.int/hiv/mediacentre/news62/en/index.html

Waldo, S. W., H. S. Rosario, A. H. Penn, and G. W. Schmid-Schonbein. 2003. Pancreatic digestive enzymes are potent generators of mediators for leukocyte activation and mortality. *Shock* 20:138-43.